

NEA NUCLEAR SCIENCE COMMITTEE
NEA COMMITTEE ON SAFETY OF NUCLEAR INSTALLATIONS

BOILING WATER REACTOR TURBINE TRIP (TT) BENCHMARK

Volume I: Final Specifications

By

Jorge Solis, Kostadin N. Ivanov, and Baris Sarikaya

Nuclear Engineering Program
The Pennsylvania State University
University Park, PA 16802, USA

Andy M. Olson and Kenneth W. Hunt

Exelon Nuclear
200 Exelon Way, KSA2-N
Kennett Square, PA 19348

February 2001

**US Nuclear Regulatory Commission
OECD Nuclear Energy Agency**

ORGANISATION FOR ECONOMIC CO-OPERATION AND DEVELOPMENT

Pursuant to Article 1 of the Convention signed in Paris on 14th December 1960, and which came into force on 30th September 1961, the Organization for Economic Co-operation and Development (OECD) shall promote policies designed:

- to achieve the highest sustainable economic growth and employment and a rising standard of living in Member countries, while maintaining financial stability, and thus to contribute to the development of the world economy;
- to contribute to sound economic expansion in Member as well as non-member countries in the process of economic development; and
- to contribute to the expansion of world trade on a multilateral, non-discriminatory basis in accordance with international obligations.

The original Member countries of the OECD are Austria, Belgium, Canada, Denmark, France, Germany, Greece, Iceland, Ireland, Italy, Luxembourg, the Netherlands, Norway, Portugal, Spain, Sweden, Switzerland, Turkey, the United Kingdom and the United States. The following countries became Members subsequently through accession at the dates indicated hereafter; Japan (28th April 1964), Finland (28th January 1969), Australia (7th June 1971), New Zealand (29th May 1973), Mexico (18th May 1994), the Czech Republic (21st December 1995), Hungary (7th May 1996), Poland (22nd November 1996) and the Republic of Korea (12th December 1996). The Commission of the European Communities takes part in the work of the OECD (Article 13 of the OECD Convention).

NUCLEAR ENERGY AGENCY

The OECD Nuclear Energy Agency (NEA) was established on 1st February 1958 under the name of OEEC European Nuclear Energy Agency. It received its present designation on 20th April 1972, when Japan became its first non-European full Member. NEA membership today consist of all OECD Member countries, except New Zealand and Poland. The Commission of the European Communities takes part in the work of the Agency.

The primary objective of the NEA is to promote co-operation among the governments of its participating countries in furthering the development of nuclear power as a safe, environmentally acceptable and economic energy source.

This is achieved by:

- *encouraging harmonization of national regulatory policies and practices, with particular reference to the safety of nuclear installations, protection of man against ionizing radiation and preservation of the environment, radioactive waste management, and nuclear third party liability and insurance;*
- *assessing the contribution of nuclear power to the overall energy supply by keeping under review the technical and economic aspects of nuclear power growth and forecasting demand and supply for the different phases of the nuclear fuel cycle;*
- *developing exchanges of scientific and technical information particularly through participation in common services;*
- *setting up international research and development programmes and joint undertakings.*

In these and related tasks, the NEA works in close collaboration with the International Atomic Energy Agency in Vienna, with which it has concluded a Co-operation Agreement, as well as with other international organisations in the nuclear field.

© OECD 2001

Permission to reproduce a portion of this work for non-commercial purposes or classroom use should be obtained through the Centre français d'exploitation du droit de copie (CCF), 20, rue des Grands-Augustins, 75006 Paris, France, Tel. (33-1) 44 07 47 70, Fax (33-1) 46 34 67 19, for every country except the United States. In the United States permission should be obtained through the Copyright Clearance Center, Customer Service, (508)750-8400, 222 Rosewood Drive, Danvers, MA 01923, USA, or CCC Online: <http://www.copyright.com/>. All other applications for permission to reproduce or translate all or part of this book should be made to OECD Publications, 2, rue André-Pascal, 75775 Paris Cedex 16, France.

FOREWORD

The Nuclear Energy Agency (NEA) of the Organization for Economic Cooperation and Development (OECD) has recently completed under the US Nuclear Regulatory Commission (NRC) sponsorship a PWR Main Steam Line (MSLB) Benchmark against coupled system thermal-hydraulic and neutron kinetics codes. A small benchmark team from the Pennsylvania State University (PSU) was responsible for developing the benchmark specification, assisting the participants and coordinating the benchmark activities. The benchmark was very well internationally accepted. It was felt among the participants that there should be a similar benchmark against the codes for a BWR plant transient. The Turbine Trip (TT) transients in a BWR are pressurization events in which the coupling between core phenomena and system dynamics plays an important role. In addition the available real plant experimental data makes the proposed benchmark problem very valuable. NEA, OECD and US NRC have approved it for the purpose of validating advanced system best-estimate analysis codes. A small team at PSU is responsible for authoring the final specifications, coordinating the benchmark activities, answering the questions, analyzing the solutions submitted by benchmark participants, and providing reports summarizing the results for each phase. In performing these tasks the PSU team is collaborating with Andy M. Olson and Kenneth W. Hunt from PECO Nuclear. Lance J. Agee, EPRI, provides technical assistance for this international benchmark project also.

Three benchmark workshops are scheduled during the course of benchmark activities. The first workshop will be conducted for the participants on the exercises of the BWR TT transient. The workshop took place November 9-10 2000 in Philadelphia and was hosted by Exelon Nuclear. The information needed for the exercises was clearly presented to the participants in order to be able to proceed with the calculations in an efficient and timely manner. The second workshop for the participants will be conducted, which will focus on resolving issues, which may have arisen in the analyses of the first two exercises. In addition any issues related to the third exercise will be discussed also. This workshop is scheduled for October 15-16 2001 and is hosted by Paul Scherrer Institut (PSI), Switzerland. Final (third) workshop on benchmark will be conducted in May 2002 to resolve issues related to the third exercise, to address any outstanding issues, and to reach an agreement on the technical basis for the final reports. It is planned to be hosted by the Institute for Safety Research, Research Center Rossendorf, Germany.

The OECD/NRC BWR TT Benchmark would be published in four volumes as OECD/NEA and NUREG/CR reports.

CD-ROMs will be prepared with the four reports and the transient boundary conditions, decay heat values, as a function of time, cross-section libraries and supplementary tables and graphs not published in the paper version. The transient boundary conditions, decay heat values and the cross-section libraries can be found also at the benchmark ftp site:

Address: varna.me.psu.edu; **Id:** bwrttp; **Password:** tt2000

Acknowledgements

The authors would like to thank Prof. J. Aragonés from UPM, Dr. T. Lefvert, Dr. S. Langenbuch from GRS, and Dr. Farouk Eltawila of US NRC, whose support and encouragement in establishing this benchmark are invaluable.

This report is the sum of many efforts, the participants, the funding agencies and their staff – the US Nuclear Regulatory Commission and the Organization of Economic Co-operation and Development. Special appreciation is given to: Lance Agee from EPRI, Prof. T. Downar from Purdue University, B. Aktas from ISLINC, Dr. G. Gose and Dr. C. Peterson from CSA, Dr. A. Hotta from TSI, Dr. P. Coddington from PSI, and Dr. U. Grundmann from FZR. Their technical assistance, comments and suggestions have been very valuable. We would like to thank them for the effort and time involved.

Of particular note are the efforts of Dr. Farouk Eltawila assisted by Dr. James Han and Dr. Jennifer Uhle of the US Nuclear Regulatory Commission. Through their efforts, funding is secured enabling this effort to proceed. We also thank them for their invaluable technical advice and assistance.

The authors wish to express their sincere appreciation for the outstanding support offered by Dr. Enrico Sartori, who is providing efficient administration, organizing and valuable technical advice.

Finally, we are grateful to Amanda Costa for having devoted her competence and skills to the editing of this report.

TABLE OF CONTENTS

FOREWORD.....	iii
Acknowledgments.....	iv
List of Figures.....	viii
List of Tables.....	ix
Chapter 1 Introduction.....	1
1.1 Objectives.....	2
1.2 Definition of benchmark exercises.....	2
1.2.1 Exercise 1 – Power vs. Time Plant System Simulation with Fixed Axial Power Profile Table.....	2
1.2.2 Exercise 2 – Coupled 3-D Kinetics/Core T-H BC model and/or 1D Kinetics Plant System Simulation.....	2
1.2.3 Exercise 3 - Best-Estimate Coupled 3D Core/T-H System Modeling.....	3
Chapter 2 Core and neutronics data.....	4
2.1 General.....	4
2.2 Core geometry and fuel assembly (FA) geometry.....	4
2.3 Neutron modeling.....	4
2.4 Two-dimensional (2-D) assembly types and three-dimensional (3-D) composition maps.....	5
2.5 Cross-section library.....	5
2.6 Monitored point and average neutron fluxes in the reactor core.....	7
2.7 Corrected average coolant density for feedback effects.....	8

Chapter 3	Thermal-hydraulic data.....	35
3.1	Component specifications for the full thermal-hydraulic system model.....	35
3.1.1	Reactor vessel.....	35
3.1.2	Reactor recirculation system.....	35
3.1.3	Core region.....	36
3.1.4	Steam lines.....	36
3.1.5	Feed water lines.....	36
3.2	Definition of the core thermal-hydraulic boundary conditions model.....	36
3.3	Thermal-physical and heat transfer specifications.....	37
3.3.1	Nuclear fuel (UO ₂ -PuO ₂) properties.....	37
3.3.2	Gas gap conductance.....	39
3.3.3	Zircaloy cladding properties.....	39
Chapter4	Neutronic/thermal-hydraulic coupling.....	51
Chapter5	TT problem.....	52
5.1	Description of TT2 scenario.....	52
5.2	Initial steady-state conditions.....	53
5.3	Transient calculations.....	53
Chapter 6	Output requested.....	61
6.1	Initial steady-state results.....	61
6.2	Transient results.....	61
6.3	Output format.....	62

REFERENCES.....	66
APPENDIX A Skeleton input deck.....	67
APPENDIX B Sample cross-section table.....	76

List of Figures

Figure 2.2.1	Reactor core cross-sectional view.....	25
Figure 2.2.2	PB2 initial fuel assembly lattice.....	26
Figure 2.2.3	PB2 reload fuel assembly lattice for 100 mil channels.....	27
Figure 2.2.4	PB2 reload fuel assembly lattice for 120 mil channels	28
Figure 2.2.5	PB2 reload fuel assembly lattice for LTA assemblies.....	29
Figure 2.4.1	PSU Control rod grouping.....	30
Figure 2.4.2	Radial distribution of assembly types.....	31
Figure 2.5.1	Fuel assembly orientation for ADF assignment.....	32
Figure 2.6.1	Core orificing and TIP arrangement.....	33
Figure 2.6.2	Elevation of core components.....	34
Figure 3.1.1.1	PB2 RETRAN T-H Model.....	47
Figure 3.1.2.1	Simplified TRAC-BF1 BWR jet pump model.....	48
Figure 3.2.1	PB2 OECD/NRC TT core boundary conditions model.....	49
Figure 3.2.2	PB2 Reactor Core T-H Channel Radial Map.....	50
Figure 5.2.1	PB2 TT2 Initial control rod pattern.....	60
Figure 5.2.2.	PB2 HZP control rod pattern.....	60
Figure 6.1	Form for axial power distribution.....	63
Figure 6.2	Form for radial power distribution.....	63
Figure A.1	RETRAN nodalization diagram.....	74

List of Tables

Table 2.2.1	PB2 Fuel Assembly Data.....	9
Table 2.2.2.1	Assembly Type 1.....	10
Table 2.2.2.2	Assembly Type 2.....	10
Table 2.2.2.3	Assembly Type 3.....	10
Table 2.2.2.4	Assembly Type 4.....	11
Table 2.2.2.5	Assembly Type 5.....	11
Table 2.2.2.6	Assembly Type 6.....	12
Table 2.3.1	Decay constant and fractions of delayed neutrons.....	12
Table 2.3.2	Heavy-element decay heat constants.....	12
Table 2.4.1.1	Bundle design for type 1 initial fuel.....	13
Table 2.4.1.2	Bundle design for type 2 initial fuel.....	14
Table 2.4.1.3	Bundle design for type 3 initial fuel.....	15
Table 2.4.1.4	Bundle design for type 4 8x8 UO ₂ reload.....	16
Table 2.4.1.5	Bundle design for type 5 8x8 UO ₂ reload.....	17
Table 2.4.1.6	Bundle design for type 6 8x8 UO ₂ reload, LTA.....	18
Table 2.4.2	Control rod data.....	19
Table 2.4.3	Definition of assembly types.....	19
Table 2.4.4	Composition numbers in axial layer for each assembly type.....	20
Table 2.5.1	Range of variables.....	21
Table 2.5.2	Key to macroscopic cross-section tables.....	22
Table 2.5.3	Macroscopic cross-section tables structure.....	22
Table 2.6.1	Measured LPRMs for levels A, B, C, and D.....	24
Table 3.1.1.1	Reactor vessel design data.....	40
Table 3.1.1.2	Peach Bottom-2 Vessel fluid volumes.....	41
Table 3.1.1.3	PB2 Reference design information.....	42
Table 3.1.2.1	Reactor recirculation system design characteristics.....	43
Table 3.1.2.2	PB2 BWR TRAC-BF1 simplified jet pump model.....	44
Table 3.1.3.1	Core related hydraulic loss coefficients (inlet orifices).....	44
Table 3.1.3.2	Fuel estimated loss coefficients.....	44
Table 3.1.3.3	Core related hydraulic leakage flows.....	45
Table 3.1.4.1	Nuclear system safety and relief valves.....	45
Table 3.1.4.2	System bypass design data.....	45
Table 3.3.3.1	Specific heat versus time for $T \leq 1248$ K.....	46
Table 5.2.1	PB2 TT2 initial conditions from process computer P1 edit.....	55
Table 5.2.2	PB2 TT2 Initial Core Axial Relative Power.....	56
Table 5.2.3	PB2 HZP initial conditions.....	56
Table 5.3.1	TSV Flow Fraction vs. Time.....	57
Table 5.3.2	Bypass Valve Position vs. Time.....	57
Table 5.3.3	Feed water Flow vs. Time.....	58
Table 5.3.4	PB2 TT2 Scram Characteristics.....	58
Table 5.3.5	CRD Position After Scram vs. Time.....	58
Table 5.3.6	PB2 TT2 Event Timing.....	59
Table 5.3.7	Peak Measured Responses.....	59
Table 5.3.8	TT2 test acquisition instrument time delays (in msec).....	59
Table 6.3.1	Sequence of events output.....	64

Chapter 1

Introduction

Incorporation of full three-dimensional (3-D) models of the reactor core into system transient codes allows for a “best-estimate” calculation of interactions between the core behavior and plant dynamics. Recent progress in the computer technology has made development of coupled system thermal-hydraulic and neutron kinetics code systems feasible. Considerable efforts have been made in various countries and organizations in this direction. To verify the capability of the coupled codes to analyze complex transients with coupled core-plant interactions and to fully test thermal-hydraulic coupling, appropriate Light Water Reactor (LWR) transient benchmarks need to be developed on a higher “best-estimate” level. The previous sets of transient benchmark problems addressed separately system transients (designed mainly for thermal-hydraulic system codes with point kinetics models) and core transients (designed for thermal-hydraulic core boundary conditions models coupled with a three-dimensional (3-D) neutron kinetics models). The Nuclear Energy Agency (NEA) of the Organization for Economic Cooperation and Development (OECD) has recently completed under the US Nuclear Regulatory Commission (NRC) sponsorship a PWR Main Steam Line (MSLB) Benchmark [1] against coupled thermal-hydraulic and neutron kinetics codes. A benchmark team from the Pennsylvania State University (PSU) has been responsible for developing the benchmark specifications, assisting the participants and coordinating the benchmark activities. The benchmark was well accepted by the international community. The participants of the PWR benchmark felt that there should be a similar benchmark against the codes for a BWR plant transient. A Turbine Trip (TT) transient in a BWR is a pressurization event in which the coupling between core phenomena and system dynamics plays an important role. In addition, the available real plant experimental data [2,3] makes the proposed benchmark problem very valuable. NEA, OECD and US NRC have approved a BWR TT benchmark for the purpose of validating advanced system best-estimate analysis codes.

As a result, this benchmark project is established to challenge the coupled system thermal-hydraulic/neutron kinetics codes against a Peach-Bottom-2 (a GE-designed BWR/4) turbine trip transient with a sudden closure of the turbine stop valve. Three-turbine trip transients at different power levels were performed at the Peach Bottom (PB)-2 BWR/4 Nuclear Power Plant (NPP) prior to shutdown for refueling at the end of Cycle 2 in April 1977. The second test is selected for the benchmark problem to investigate the effect of the pressurization transient, (following the sudden closure of the turbine stop valve) on the neutron flux in the reactor core. In a best-estimate manner the test conditions approached the design basis conditions as closely as possible. The actual data were collected, including a compilation of reactor design and operating data for Cycles 1 and 2 of PB and the plant transient experimental data. The transient was selected for this benchmark, because it is a dynamically complex event for which neutron kinetics in the core was coupled with thermal-hydraulics in the reactor primary system.

1.1 Objectives

The BWR reference problem chosen for simulation is a Turbine Trip transient, which begins with a sudden Turbine Stop Valve (TSV) closure. The pressure oscillation generated in the main steam piping propagates with relatively little attenuation into the reactor core. The induced core pressure oscillation results in dramatic changes of the core void distribution and fluid flow. The magnitude of the neutron flux transient taking place in the BWR core is strongly affected by the initial rate of pressure rise caused by pressure oscillation and has a strong spatial variation. The correct simulation of the power response to the pressure pulse and subsequent void collapse requires a 3-D core modeling supplemented by a one-dimensional (1-D) simulation of the remainder of the reactor coolant system.

The purpose of this proposal is to establish a BWR TT benchmark exercise, based on a well defined problem with complete set of input specifications and reference experimental data, for qualification of the coupled 3-D neutron kinetics/thermal-hydraulic system transient codes. Since this kind of transient is a dynamically complex event with reactor variables changing very rapidly, it constitutes a good benchmark problem to test the coupled codes on both levels: neutronics/thermal-hydraulic coupling and core/plant system coupling. Subsequently, the objectives of the proposed benchmark are: comprehensive feedback testing and examination of the capability of coupled codes to analyze complex transients with coupled core/plant interactions by comparison with actual experimental data.

1.2 Definition of the benchmark exercises

The benchmark consists of three separate exercises:

1.2.1 Exercise 1 - Power vs. Time Plant System Simulation with Fixed Axial Power Profile Table (Obtained from Experimental Data)

The purpose of the first exercise is to test the thermal-hydraulic system response and to initialize the participants' system models. Core power response is fixed to reproduce the actual test results utilizing either power or reactivity vs. time data.

1.2.2 Exercise 2 - Coupled 3-D Kinetics/Core Thermal-Hydraulic BC Model and/or 1-D Kinetics Plant System Simulation

Two steady states are to be modeled for Exercise 2: Hot Zero Power (HZP) conditions and the initial conditions of TT2. The HZP state would provide a clean initialization of the core neutronics models since the thermal-hydraulic feedback is spatially uniform across the core. The description of HZP conditions is provided later in Chapter 3 of the Specifications.

The second exercise consists of two options. Option 1 of the second exercise is to perform a coupled 3-D kinetics/thermal-hydraulic calculation for the reactor core using the PSU-provided boundary conditions at core inlet and exit. The core boundary conditions will be provided utilizing a combination of the calculated PSU results and test data. Option 2 of the second exercise is to perform coupled 1-D neutron kinetics/thermal-hydraulics core boundary condition model calculation for the core using the same boundary conditions provided for option 1. 1-D cross-sections are collapsed from the cross-section libraries generated for 3-D simulation. The participants can participate in either or both options.

1.2.3 Exercise 3 - Best-Estimate Coupled 3-D Core/Thermal-Hydraulic System Modeling

The third exercise consists also of 2 options. In Option 1 the participants perform a coupled 3-D core/thermal-hydraulic calculation for the core and 1-D thermal-hydraulics modeling for the balance of the plant. In option 2 the participants perform the calculation using a 1-D kinetics core model and 1-D thermal-hydraulics for the reactor primary system. This exercise combines elements of the first two exercises of this benchmark and is an analysis of the transient in its entirety.

Extreme versions of Exercise 3, that provide the opportunity to test better the code coupling and feedback modeling are defined as follows:

1. Turbine trip without bypass system relief opening (would increase the power peak and provide enough pressurization for safety/relief valve opening).
2. Turbine trip without scram (would increase the power peak and produce a second power peak and would be a challenge to the coupled code predictions).
3. Combined extreme scenario – turbine trip with bypass system relief failure and without reactor scram. Some preliminary results indicate that this case is very close to a super-prompt-critical state and makes a good case for code-to-code comparisons.

The initial steady-state reference results will be based on those provided from the P-1 process computer power distribution data in the EPRI reports [2]. For the TT2 transient test [3], the dynamic measurements were taken with high-speed digital acquisition system capable of sampling over 150 signals every 6 milliseconds. The core power distribution measurements were taken from the plant's local in-core flux detectors. Special fast response pressure and differential pressure transducers were installed in parallel with the existing plant instruments in the nuclear steam supply system. The TT transient scenario is based on the TT2 test, as discussed in the reference EPRI reports. In this TT transient, the nuclear power is driven by the increase in pressure, which causes a void collapse in the core. The positive power response is almost immediate, but the transient is soon slowed down by the feedback from the increased direct and conducted heat flux to the coolant, which will, in turn, produce void and give a negative reactivity feedback. The scram is triggered at a defined power level (as a multiple of the initial power). Since the transient is fast and of short duration, the fuel temperature rise is moderate and the Doppler effect plays a subordinate role, compared to other feedback effects. The complete TT scenario is described together with a set of initial and boundary conditions in Chapter 5. Transient simulations will be initiated from zero to 5 seconds, and within this time, the sequence of events, core exit pressure response, total core power response, and other integral parameters will be compared to the experimental data. For the extreme versions of Exercise 3, transient simulations should be performed for 10 seconds to capture the thermal-hydraulic response of these cases. The radial and axial power distributions at different detector levels and positions will be also compared. In addition there also will be some code-to-code comparisons for the transient behavior of other key thermal-hydraulic parameters as core average fuel temperature and core average void fraction as well as 2-D Normalized Power (NP) distribution and core average axial power distribution.

CHAPTER 2.0

Core and neutronic data

2.1 General

The reference design for the BWR is derived from real reactor, plant and operation data for the PB-2 BWR/4 NPP and it is based on the information provided in the EPRI reports and some additional sources such as the PECO Energy Topical Report [4]. This chapter specifies the core and neutronic data to be used in all the calculations.

2.2 Core geometry and fuel assembly (FA) geometry

The radial geometry of the reactor core is shown in Figure 2.2.1. Radially, the core is divided into cells 15.24 cm wide, each corresponding to one fuel assembly (FA), plus a radial reflector (shaded area of Figure 2.2.1) of the same width. There are a total of 888 assemblies, 764 FA and 124 reflector assemblies. Axially, the reactor core is divided into 26 layers (24 core layers plus top and bottom reflectors) with a constant height of 15.24 cm (including reflector nodes). The total active core height is 365.76 cm. The axial nodalization accounts for material changes in the fuel design and for exposure and history variations. Geometric data for the FA and fuel rod is provided in Table 2.2.1. Data for different assembly designs is given in Table 2.2.2.1 through Table 2.2.2.6. Fuel assembly lattice drawings, including detailed dimensions, for initial fuel, reload fuel with 100 and 120 mil channels, and the lead test assemblies (LTA) are shown in Figures 2.2.2 through 2.2.5. The numbers 100 and 120 refer to the wall thickness of the channel (1 mil = 0.001 inches).

The core loading during the test was as follows: 576 fuel assemblies were the original 7x7 type from cycle 1 (C1), and the remaining 188 were a reload of 8x8 fuel assemblies. One hundred and eighty-five control rods provided reactivity control. To build the participant's given neutronic model, these control rods can be grouped according to their initial insertion position (see Chapter 5, Figure 5.2.1). The control rod grouping used by PSU to perform reference calculations is presented in figure 2.4.1.

2.3 Neutron modelling

Two prompt and six delayed neutron groups are modelled. The energy release per fission for the two prompt neutron groups is 0.3213×10^{-10} and 0.3206×10^{-10} W-s/fission, and this energy release is considered to be independent of time and space. It is assumed that 2% of fission power is released as direct gamma heating for the in-channel coolant flow and 1.7% for the bypass flow.

Table 2.3.1 shows global core-wide decay time constants and fractions of delayed neutrons. In addition delayed parameters are provided in the cross-section library for each of the composition shown in Table 2.4.4.

It is recommended that ANS-79 be used as a decay heat standard model. In total 71 decay-heat groups are used: 69 groups are used for the three isotopes ^{235}U , ^{239}Pu and ^{238}U with the decay-heat constants defined in the 1979 ANS standard; plus, the heavy-element decay heat groups for ^{239}U and ^{239}Np are used with constants given in Table 2.3.2. It is recommended that the participants also use the assumption of an infinite operation at a power of 3293 MWt. For participants who are not capable of using the ANS-79 decay heat standard, a file of the decay heat evolution throughout the transient is provided on CD-ROM and at the benchmark **ftp** site under the directory **Decay-Heat**. These predictions are obtained using the Pennsylvania State University (PSU) coupled code results. The effective decay heat energy fraction of the total thermal power (the relative contribution in the steady state) is equal to 0.065583.

2.4 Two-dimensional (2-D) assembly types and three-dimensional (3-D) composition maps

Nineteen assembly types are contained within the core geometry. There are 435 compositions. The corresponding sets of cross-sections are provided. Each composition is defined by material properties (due to changes in the fuel design) and burn-up. The burn-up dependence is a three-component vector of variables: exposure (GWd/t), spectral history (void fraction), and control rod history. Assembly designs are defined in Tables 2.4.1.1 through 2.4.1.6. Control rod geometry data is provided in Table 2.4.2. The definition of assembly types is shown in Table 2.4.3. The radial distribution of these assembly types, within the reactor geometry is shown in Figure 2.4.2. The axial locations of compositions for each assembly type are shown in Table 2.4.4.

2.5 Cross-section library

A complete set of diffusion coefficients, macroscopic cross-sections for scattering, absorption, and fission, assembly discontinuity factors (ADFs), as a function of the moderator density and fuel temperature is defined for each composition. The group inverse neutron velocities are also provided for each composition. Dependence of the cross-sections on the above variables is specified through a two-dimensional table look-up. Each composition is assigned to a cross-section set containing separate tables for the diffusion coefficients and cross-sections, with each point in the table representing a possible core state. The expected range of the transient is covered by the selection of an adequate range for the independent variables shown in Table 2.5.1. Specifically, Exercise 1 was used for selecting the range of thermal-hydraulic variables. A steady state calculation was run using the TRAC-BF1 code and initial conditions of turbine trip 2 for choosing discrete values of the thermal-hydraulic variables (pressure, void fraction, and coolant/moderator temperature). A transient calculation was performed to find out the expected range of change of the above variables.

A modified linear interpolation scheme (which includes extrapolation outside the thermal-hydraulic range) is used to obtain the appropriate total cross-sections from the tabulated ones based on the reactor conditions being modelled. Table 2.5.2 shows the definition of a cross-section table associated with a composition. Table 2.5.3 shows the macroscopic cross-section table structure for one cross-section set. All cross-section sets are assembled into a cross-section

library. The cross-sections are provided in separate libraries for rodded (**nemtabr**) and unrodded compositions (**nemtab**). The format of each library is as follows:

- The first line of data is used to show the number of data points used for the independent thermal-hydraulic parameters. The parameters used in this benchmark include fuel temperature, moderator density.
- Each cross-section set is in the order shown in Table 2.5.3. Each table is in the format described in Table 2.5.2. More detailed information on this format is presented in Appendix B. First, the values of the independent thermal-hydraulic parameters (fuel temperature and moderator density) used to specify that particular set of cross-sections are listed, followed by the values of the cross-sections** and ADFs. Since there is one-half symmetry for all the assembly designs, two ADFs per composition per energy group are provided – West (wide gap) and South (narrow gap). Because the fuel assembly designs employed in PB-2 core design have one-half symmetry, the following assumption is made: North is equal to West and East is equal to South (e.g., Figure 2.5.1). Detector parameters*** are included after the two-group cross-sections followed by the delayed neutron parameters for six groups. Finally, the group inverse neutron velocities complete the data for a given cross-section set.
- The dependence on fuel temperature in the reflector cross-section tables is also modelled. This is because the reflector cross-sections are generated by performing lattice physics transport calculations, including the next fuel region. In order to simplify the reflector feedback modelling the following assumptions are made for this benchmark: an average fuel temperature value equal to 550 K is used for the radial reflector cross-section modelling in both the initial steady-state and transient simulations, and the average coolant density for the radial reflector is equal to the inlet coolant density. For the axial reflector regions the following assumptions are made: for the bottom – the fuel temperature is equal to the inlet coolant temperature (per thermal-hydraulic channel or cell) and the coolant density is equal to the inlet coolant density (again per channel); for the top – the fuel temperature is equal to the outlet coolant temperature (per channel) and the coolant density is equal to the outlet coolant density (per channel).

All cross-section data, along with a program for linear interpolation, are supplied on CD-ROM and at the benchmark **ftp** site under the directory **XS-Lib** in the format described above.

For the generation of 1-D cross-sections, each plane is treated as a different composition and each planar cross section is obtained from a 3-D coupled code steady-state calculation. Since these cross sections are functions of thermal-hydraulic state parameters such as moderator density and fuel temperature, several 3-D calculations are performed to generate planar cross sections at various thermal-hydraulic states in order to cover the range of thermal-hydraulic conditions encountered under the simulated transient. The planar cross sections are then functionalised for the use of 1-D calculations. Two cross-section libraries for both TRAC and RETRAN 1-D cross-section formats are generated for performing 1-D kinetics calculations. These libraries are also located at the benchmark site under XS-Lib directory. They are also provided on the CD-ROM.

** Please note that the provided absorption cross-sections already take the xenon thermal cross-sections into account; however, at the participants' request, the thermal macro and micro xenon cross-sections are listed in the cross-section sets.

*** Detector parameters are described in Section 2.6

2.6 Monitored and average neutron fluxes in the reactor core

BWR LPRM Response Model

For the purpose of comparing the three-dimensional (3-D) power distribution provided experimentally by local power range monitor (LPRM) measurements during PB2 TT2, the following LPRM response model could be implemented in the 3-D neutronics code:

$$R_{\text{LPRM}}(x, y, z) = \sum_{g=1}^2 \phi_g^{\text{global}}(x, y, z) \cdot \phi_g^{\text{bundle}}(x, y, z) \cdot \sigma_g^{\text{detector}}$$

Where

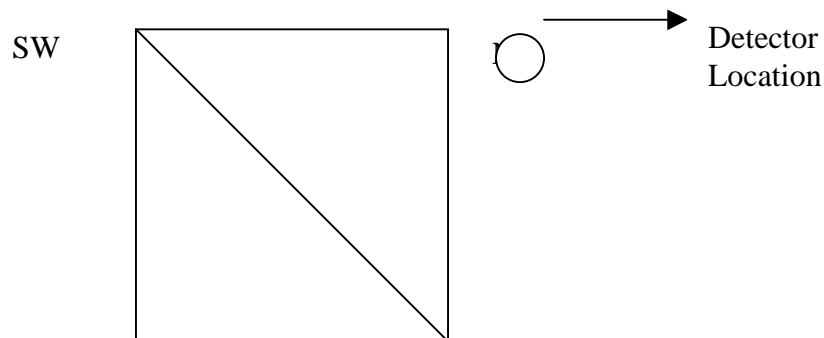
$\phi_g^{\text{global}}(x, y, z)$ is the homogeneous flux from the 3-D kinetics global solution extrapolated at the detector location at the detector location. It could be obtained from the global core neutronics calculation by extrapolating the flux function to the detector location based on the specific code solution method.

$\phi_g^{\text{bundle}}(x, y, z)$ is the single assembly detector factor which is the ratio between the flux in the detector location and the average flux of the neutronic cell (from lattice CASMO calculation):

$$\phi_g^{\text{bundle}}(x, y, z) = \frac{\phi^{\text{detector, lattice}}(x, y, z)}{\phi_g^{\text{avg, lattice}}}$$

$\sigma_g^{\text{detector}}$ is the microscopic fission cross section for fissile material of the fission chamber.

Microscopic cross-sections of the fission material and the detector factors are provided in cross-section tables as is it described in Section 2.5. The detector responses of the surrounding four neutronic nodes are derived independently and then averaged. The CASMO lattice calculation uses U-235 as the fission chamber fissile material. By default, the detector position is in the South-East (SE) corner of the fuel assembly as shown below:



Experimental flux measurements

The PB2 reactor core is equipped with local neutron flux measurement instruments that are called local power range monitors (LPRMs). There are a total of 43 instrument tubes that are located radially according to Figure 2.6.1. Within each instrument tube, the LPRMs are located at 4 axial levels: Level A, Level B, Level C, and Level D which are axially located from bottom to top of the active fuel length at 18, 54, 90, and 120 inches respectively. The axial location of the above levels is shown in figure 2.6.2. Coordinates for radial location are presented in Table 2.6.1. The pair of numbers shown in Table 2.6.1 represents the (X,Y) location in a Cartesian coordinate system as it is shown in Figure 2.6.1. There were a total of 80 monitored points (20 per each axial level) during TT2 transient. Therefore, comparisons can be performed between local experimental measured fluxes and code predictions as the average of each axial Level (A, B, C, and D)

2.7 Corrected average coolant density for feedback effects

Lattice physics calculations are performed by homogenizing the fuel lattice and the bypass flow associated with it. When obtaining the average coolant density, a correction that accounts for the bypass channel conditions should be included since this is going to influence the feedback effect on the cross-section calculation through the average coolant density. The following approach should be applied:

$$\rho_{act}^{eff} = \frac{A_{act}\rho_{act} + A_{byp}(\rho_{byp} - \rho_{sat})}{A_{act}}$$

Where

ρ_{act}^{eff} is the effective average coolant density for cross-section calculation

ρ_{byp} is the average moderator coolant density of the bypass channel

ρ_{sat} is the saturated moderator coolant density of the bypass channel

A_{act} is flow cross-sectional area of the active heated channel

A_{byp} is the flow cross-sectional area of the bypass channel

Bypass conditions should be obtained by adding a bypass channel to represent by core bypass region in the thermal0hydraulic model.

Table 2.2.1 PB2 Fuel Assembly Data

	Initial Load			Reload	Reload	LTA Special
Assembly Type	1	2	3	4	5	6
No. of Assemblies, Initial Core	168	263	333	0	0	0
No. of Assemblies, C2 Geometry	0 7x7	261 7x7	315 7x7	68 8x8	116 8x8	4 8x8
Assembly Pitch, in	6.0	6.0	6.0	6.0	6.0	6.0
Fuel Rod Pitch	0.738	0.738	0.738	0.640	0.640	0.640
Fuel Rods per Assembly	49	49	49	63	63	62
Water Rods per Assembly	0	0	0	1	1	2
Burnable Poison Positions	0	4	5	5	5	5
No. of Spacer Grids	7	7	7	7	7	7
Inconel per Grid, lb	0.102	0.102	0.102	0.102	0.102	0.102
Zr-4 per Grid, lb	0.537	0.537	0.537	0.614	0.614	0.614
Spacer Width, in	1.625	1.625	1.625	1.625	1.625	1.625
Assembly Average Fuel Composition:						
Gd ₂ O ₃ , g	0	441	547	490	328	313
UO ₂ , kg	222.44	212.21	212.06	207.78	208.0	207.14
Total Fuel, kg	222.44	212.65	212.61	208.27	208.33	207.45

Table 2.2.2.1 Assembly Design 1							
Rod Type	Number of Rods	Pellet Density		Stack Density (g/cm ³)	Gd ₂ O ₃ (g)	UO ₂ (g)	Stack Length (cm)
		UO ₂ (g/cm ³)	UO ₂ +Gd ₂ O ₃ (g/cm ³)				
1	31	10.42		10.34	0	4548	365.76
2	17	10.42		10.34	0	4548	365.76
2s	1	10.42		10.34	0	4140	330.2
Pellet outer diameter = 1.23698 cm Cladding = Zircaloy-2, 1.43002 cm outer diameter x .08128 cm wall thickness, all rods Gas plenum length = 40.64 cm							

Table 2.2.2.2 Assembly Design 2							
Rod Type	Number of Rods	Pellet Density		Stack Density (g/cm ³)	Gd ₂ O ₃ (g)	UO ₂ (g)	Stack Length (cm)
		UO ₂ (g/cm ³)	UO ₂ +Gd ₂ O ₃ (g/cm ³)				
1	25	10.42	--	10.32	0	4352	365.76
1s	1	10.42	--	10.32	0	3935	330.2
2	12	10.42	--	10.32	0	4352	365.76
3	6	10.42	--	10.32	0	4352	365.76
4	1	10.42	--	10.32	0	4352	365.76
5A	3	--	10.29	10.19	129	4171	365.76
6B	1	10.42	10.29	10.27	54	4277	365.76
Pellet outer diameter = 1.21158 cm Cladding = Zircaloy-2, 1.43002 cm outer diameter x .09398 cm wall thickness, all rods Gas plenum length = 40.132 cm							

Table 2.2.2.3 Assembly Design 3							
Rod Type	Number of Rods	Pellet Density		Stack Density (g/cm ³)	Gd ₂ O ₃ (g)	UO ₂ (g)	Stack Length (cm)
		UO ₂ (g/cm ³)	UO ₂ +Gd ₂ O ₃ (g/cm ³)				
1	26	10.42	--	10.32	0	4352	365.76
2	11	10.42	--	10.32	0	4352	365.76
3	6	10.42	--	10.32	0	4352	365.76
4	1	10.42	--	10.32	0	4352	365.76
5A	2	--	10.29	10.19	129	4171	365.76
6C	1	--	10.29	10.19	117	3771	330.20
7E	1	10.42	10.25	10.28	43	4292	365.76
8D	1	10.42	10.25	10.19	129	4172	365.76
Pellet outer diameter = 1.21158 cm Cladding = Zircaloy-2, 1.43002 cm outer diameter x .09398 cm wall thickness, all rods Gas plenum length = 40.132 cm							

Table 2.2.2.4 Assembly Design 4							
Rod Type	Number of Rods	Pellet Density		Stack Density (g/cm ³)	Gd ₂ O ₃ (g)	UO ₂ (g)	Stack Length (cm)
		UO ₂ (g/cm ³)	UO ₂ +Gd ₂ O ₃ (g/cm ³)				
1	39	10.42	--	10.32	0	3309	365.76
2	14	10.42	--	10.32	0	3309	365.76
3	4	10.42	--	10.32	0	3309	365.76
4	1	10.42	--	10.32	0	3309	365.76
5	5	--	10.29	10.19	98	3172	365.76
WS	1	--	--	--	0	0	--

Pellet outer diameter = 1.05664 cm
 Cladding = Zircaloy-2, 1.25222 cm outer diameter x .08636 cm wall thickness, all rods
 Gas plenum length = 40.64 cm except water rod
 Gd₂O₃ in rod type 5 runs full 365.76 cm
 Water rod (WS) has holes drilled top and bottom to provide water flow and little or no boiling
 Water rod is also a spacer positioning rod

Table 2.2.2.5 Assembly Design 5							
Rod Type	Number of Rods	Pellet Density		Stack Density (g/cm ³)	Gd ₂ O ₃ (g)	UO ₂ (g)	Stack Length (cm)
		UO ₂ (g/cm ³)	UO ₂ +Gd ₂ O ₃ (g/cm ³)				
1	39	10.42	--	10.32	0	3309	365.76
2	14	10.42	--	10.32	0	3309	365.76
3	4	10.42	--	10.32	0	3309	365.76
4	1	10.42	--	10.32	0	3309	365.76
5	5	--	10.33	10.23	66	3216	365.76
WS	1	--	--	--	0	0	--

Pellet outer diameter = 1.05664 cm
 Cladding = Zircaloy-2, 1.25222 cm outer diameter x .08636 cm wall thickness, all rods
 Gas plenum length = 40.64 cm, except water rod
 Gd₂O₃ in rod type 5 runs full 365.76 cm
 Water rod (WS) has holes drilled top and bottom to provide water flow and little or no boiling
 Water rod is also a spacer positioning rod

Rod Type	Number of Rods	Pellet Density		Stack Density (g/cm ³)	Gd ₂ O ₃ (g)	UO ₂ (g)	Stack Length (cm)
		UO ₂ (g/cm ³)	UO ₂ +Gd ₂ O ₃ (g/cm ³)				
1	38	10.42	--	10.32	0	3125	355.6
2	14	10.42	--	10.32	0	3125	355.6
3	4	10.42	--	10.32	0	3125	355.6
4	1	10.42	--	10.32	0	3125	355.6
5	5	--	10.33	10.23	63	3037	355.6
WR,WS	2	--	--	--	0	0	--
ENDS	62	10.42	--	10.32	0	223	25.4

Pellet outer diameter = 1.0414 cm
Cladding = Zircaloy-2, 1.22682 cm outer diameter x .08128 cm wall thickness, all fueled rods
= Zircaloy-2, 1.50114 cm outer diameter x .07620 cm wall thickness, water rods
Gas plenum length = 24.0792 cm
Gd₂O₃ in rod type 5 runs full 355.6 cm
Water rod (WS) has holes drilled top and bottom to provide water flow and little or no boiling
Water rod is also a spacer positioning rod

Table 2.3.1 Decay constant and fractions of delayed neutrons

Group	Decay constant (s ⁻¹)	Relative fraction of delayed neutrons in %
1	0.012813	0.0167
2	0.031536	0.1134
3	0.124703	0.1022
4	0.328273	0.2152
5	1.405280	0.0837
6	3.844728	0.0214

Total fraction of delayed neutrons: 0.5526 %

Table 2.3.2 Heavy-element decay heat constants

Group no. (isotope)	Decay constant (s ⁻¹)	Available energy from a single atom (MeV)
70 (²³⁹ U)	4.91×10^{-4}	0.474
71 (²³⁹ Np)	3.41×10^{-6}	0.419

WIDE-WIDE CORNER

2	1	1	1	1	1	1
1	1	1	2	1	1	1
1	1	2	2	2	2	1
1	2	2	2	2	2	1
1	1	2	2	2	2	1
1	1	2	2	2	1	1
1	1	1	1	1	1	1

Table 2.4.1.1 Assembly design for type 1 initial fuel

ROD TYPE	U-235 (wt%)	Gd ₂ O ₃ (wt%)	NO. OF RODS
1	1.33	0	31
2	0.71	0	18

WIDE-WIDE CORNER

4	3	3	2	2	2	3
3	2	1	1	1	1	2
3	1	5A	1	1	5A	1
2	1	1	1	1	1	1
2	1	1	1	6B	1	1
2	1	5A	1	1	1	2
3	2	1	1	1	2	2

Table 2.4.1.2 Assembly design for type 2 initial fuel

ROD TYPE	U-235 (wt%)	Gd ₂ O ₃ (wt%)	NO. OF RODS
1	2.93	0	26
2	1.94	0	12
3	1.69	0	6
4	1.33	0	1
5A	2.93	3.0	3
6B	2.93	3.0	1

WIDE-WIDE CORNER

4	3	3	2	2	2	3
3	8D	1	1	1	1	2
3	1	1	1	1	5A	1
2	1	1	6C	1	1	1
2	1	1	1	1	1	1
2	1	5A	1	1	7E	2
3	2	1	1	1	2	2

Table 2.4.1.3 Assembly design for type 3 initial fuel

ROD TYPE	U-235 (wt%)	Gd ₂ O ₃ (wt%)	NO. OF RODS
1	2.93	0	26
2	1.94	0	11
3	1.69	0	6
4	1.33	0	1
5A	2.93	3.0	2
6C	2.93	3.0	1
7E	2.93	4.0	1
8D	1.94	4.0	1

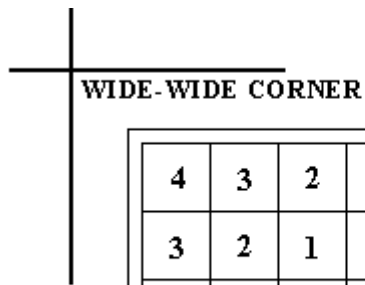
WIDE-WIDE CORNER

4	3	2	2	2	2	2	3
3	2	1	5 ^G	1	1	1	2
2	1	1	1	1	1	5 ^G	1
2	5 ^G	1	1	1	1	1	1
2	1	1	1	WS	1	1	1
2	1	1	1	1	1	1	1
2	1	5 ^G	1	1	1	5 ^G	1
3	2	1	1	1	1	1	2

Table 2.4.1.4 Assembly design for type 4 8x8 UO₂ reload

ROD TYPE	U-235 (wt%)	Gd ₂ O ₃ (wt%)	NO. OF RODS
1	3.01	0	39
2	2.22	0	14
3	1.87	0	4
4	1.45	0	1
5	3.01	3.0	5
WS	--	0	1

WS – Spacer positioning water rod
G – gadolinium rods

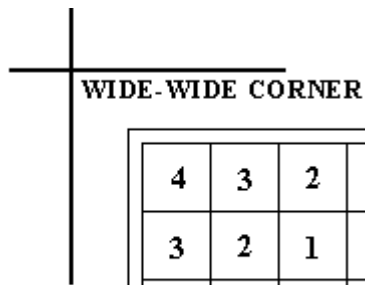


4	3	2	2	2	2	2	3
3	2	1	5 ^G	1	1	1	2
2	1	1	1	1	1	5 ^G	1
2	5 ^G	1	1	1	1	1	1
2	1	1	1	WS	1	1	1
2	1	1	1	1	1	1	1
2	1	5 ^G	1	1	1	5 ^G	1
3	2	1	1	1	1	1	2

Table 2.4.1.5 Assembly design for type 5 8x8 UO₂ reload

ROD TYPE	U-235 (wt%)	Gd ₂ O ₃ (wt%)	NO. OF RODS
1	3.01	0	39
2	2.22	0	14
3	1.87	0	4
4	1.45	0	1
5	3.01	2.0	5
WS	--	0	1

WS – Spacer positioning water rod
G – Gadolinium rods



4	3	2	2	2	2	2	3
3	2	1	5 ^G	1	1	1	2
2	1	1	1	1	1	5 ^G	1
2	5 ^G	1	1	WR	1	1	1
2	1	1	WS	1	1	1	1
2	1	1	1	1	1	1	1
2	1	5 ^G	1	1	1	5 ^G	1
3	2	1	1	1	1	1	2

Table 2.4.1.6 Assembly design for type 6 8x8 UO₂ reload, LTA

ROD TYPE	U-235 (wt%)	Gd ₂ O ₃ (wt%)	NO. OF RODS
1	3.01	0	38
2	2.22	0	14
3	1.87	0	4
4	1.45	0	1
5	3.01	2.0	5
WS	--	0	1
WR	--	0	1

WS – Spacer positioning water rod
WR – Water rod
G – Gadolinium rods

Table 2.4.2 Control rod data (Movable control rods)	
Shape	Cruciform
Pitch, cm	30.48
Stroke, cm	365.76
Control length, cm	363.22
Control material	B ₄ C granules in Type-304, stainless steel tubes and sheath
Material density	70% of theoretical
Number of control material tubes per rod	84
Tube dimensions	.47752 cm outer diameter by .0635 cm wall
Control blade half span, cm	12.3825
Control blade full thickness, cm	.79248
Control blade tip radius, cm	.39624
Sheath thickness, cm	.14224
Central structure wing length, cm	1.98501
Blank tubes per wing	None

Table 2.4.3 Definition of assembly types

Assembly Type	Assembly Design (see Tables 2.4.1.1 through 2.4.1.6)
1	5
2	4
3	5
4	6
5	2
6	2
7	2
8	2
9	2
10	2
11	3
12	2
13	3
14	2
15	3
16	2
17	3
18	2
19	reflector

Table 2.4.4 Composition numbers in axial layer for each assembly type

	1	2	3	4	5	6	7	8	9	10	11	12	13	14	15	16	17	18	19	
Bottom																				
1	433	433	433	433	433	433	433	433	433	433	433	433	433	433	433	433	433	433	433	433
2	1	25	49	73	97	121	145	169	193	217	241	265	289	313	337	361	385	409	435	435
3	2	26	50	74	98	122	146	170	194	218	242	266	290	314	338	362	386	410	435	435
4	3	27	51	75	99	123	147	171	195	219	243	267	291	315	339	363	387	411	435	435
5	4	28	52	76	100	124	148	172	196	220	244	268	292	316	340	364	388	412	435	435
6	5	29	53	77	101	125	149	173	197	221	245	269	293	317	341	365	389	413	435	435
7	6	30	54	78	102	126	150	174	198	222	246	270	294	318	342	366	390	414	435	435
8	7	31	55	79	103	127	151	175	199	223	247	271	295	319	343	367	391	415	435	435
9	8	32	56	80	104	128	152	176	200	224	248	272	296	320	344	368	392	416	435	435
10	9	33	57	81	105	129	153	177	201	225	249	273	297	321	345	369	393	417	435	435
11	10	34	58	82	106	130	154	178	202	226	250	274	298	322	346	370	394	418	435	435
12	11	35	59	83	107	131	155	179	203	227	251	275	299	323	347	371	395	419	435	435
13	12	36	60	84	108	132	156	180	204	228	252	276	300	324	348	372	396	420	435	435
14	13	37	61	85	109	133	157	181	205	229	253	277	301	325	349	373	397	421	435	435
15	14	38	62	86	110	134	158	182	206	230	254	278	302	326	350	374	398	422	435	435
16	15	39	63	87	111	135	159	183	207	231	255	279	303	327	351	375	399	423	435	435
17	16	40	64	88	112	136	160	184	208	232	256	280	304	328	352	376	400	424	435	435
18	17	41	65	89	113	137	161	185	209	233	257	281	305	329	353	377	401	425	435	435
19	18	42	66	90	114	138	162	186	210	234	258	282	306	330	354	378	402	426	435	435
20	19	43	67	91	115	139	163	187	211	235	259	283	307	331	355	379	403	427	435	435
21	20	44	68	92	116	140	164	188	212	236	260	284	308	332	356	380	404	428	435	435
22	21	45	69	93	117	141	165	189	213	237	261	285	309	333	357	381	405	429	435	435
23	22	46	70	94	118	142	166	190	214	238	262	286	310	334	358	382	406	430	435	435
24	23	47	71	95	119	143	167	191	215	239	263	287	311	335	359	383	407	431	435	435
25	24	48	72	96	120	144	168	192	216	240	264	288	312	336	360	384	408	432	435	435
26	434	434	434	434	434	434	434	434	434	434	434	434	434	434	434	434	434	434	434	434
Top																				

Table 2.5.1 Range of variables

T Fuel (°K)	Rho M. (kg/m³)
400.0	141.595
800.0	141.595
1200.0	141.595
1600.0	141.595
2000.0	141.595
2400.0	141.595
400.0	226.154
800.0	226.154
1200.0	226.154
1600.0	226.154
2000.0	226.154
2400.0	226.154
400.0	299.645
800.0	299.645
1200.0	299.645
1600.0	299.645
2000.0	299.645
2400.0	299.645
400.0	435.045
800.0	435.045
1200.0	435.045
1600.0	435.045
2000.0	435.045
2400.0	435.045
400.0	599.172
800.0	599.172
1200.0	599.172
1600.0	599.172
2000.0	599.172
2400.0	599.172
400.0	779.405
800.0	779.405
1200.0	779.405
1600.0	779.405
2000.0	779.405
2400.0	779.405

Table 2.5.2 Key to macroscopic cross-section tables

T_{f1}	T_{f2}	T_{f3}	T_{f4}	T_{f5}	T_{f6}
ρ_{m1}	ρ_{m2}	ρ_{m3}	ρ_{m4}	ρ_{m5}	ρ_{m6}
Σ_1	Σ_2	...			
		...	Σ_{34}	Σ_{35}	Σ_{36}

Where:

– T_f is the Doppler (fuel) temperature ($^{\circ}\text{K}$)

– ρ_m is the moderator density (kg/m^3)

Macroscopic cross-sections are in units of cm^{-1}

Table 2.5.3 Macroscopic cross-section tables structure

```

*****
Cross-Section Table Input
*
*      T Fuel      Rho Mod.
*          6          6
*
***** X-Section Set #
#
*****
Group No. 1
*
***** Diffusion Coefficient Table
*
***** Absorption X-Section Table
*
***** Fission X-Section Table
*
***** Nu-Fission X-Section Table
*
***** Scattering From Group 1 to 2 X-Section Table
*
***** Assembly Disc. Factor Table - W
*
***** Assembly Disc. Factor Table - S
*
*****
Group No. 2
*
***** Diffusion Coefficient Table

```

```

*
***** Absorption X-Section Table
*
***** Fission X-Section Table
*
***** Nu-Fission X-Section Table
*
***** Xe Macroscopic X-Section Table
*
***** Xe Microscopic X-Section Table
*
***** Assembly Disc. Factor Table - W
*
***** Assembly Disc. Factor Table - S
*
***** Detector Flux Ratio Table (not energy group dependent)
*
***** Detector Microscopic Fission X-Section Table (not energy group dependent)
*
***** Effective Delayed Neutron Yield in Six Groups
*
***** Decay Constants for Delayed Neutron Groups
*
***** Inv. Neutron Velocities
*

```


Table 2.6.1 Measured LPRMs for levels A, B, C, and D

Coordinates for radial location (see Figure 5.4.2)

08-17
08-25
08-33
08-49
16-33
16-49
16-57
24-17
24-25
24-41
32-09
32-33
32-41
32-57
40-33
40-41
48-25
48-49
56-25
56-33

Figure 2.2.1 Reactor core cross-sectional view

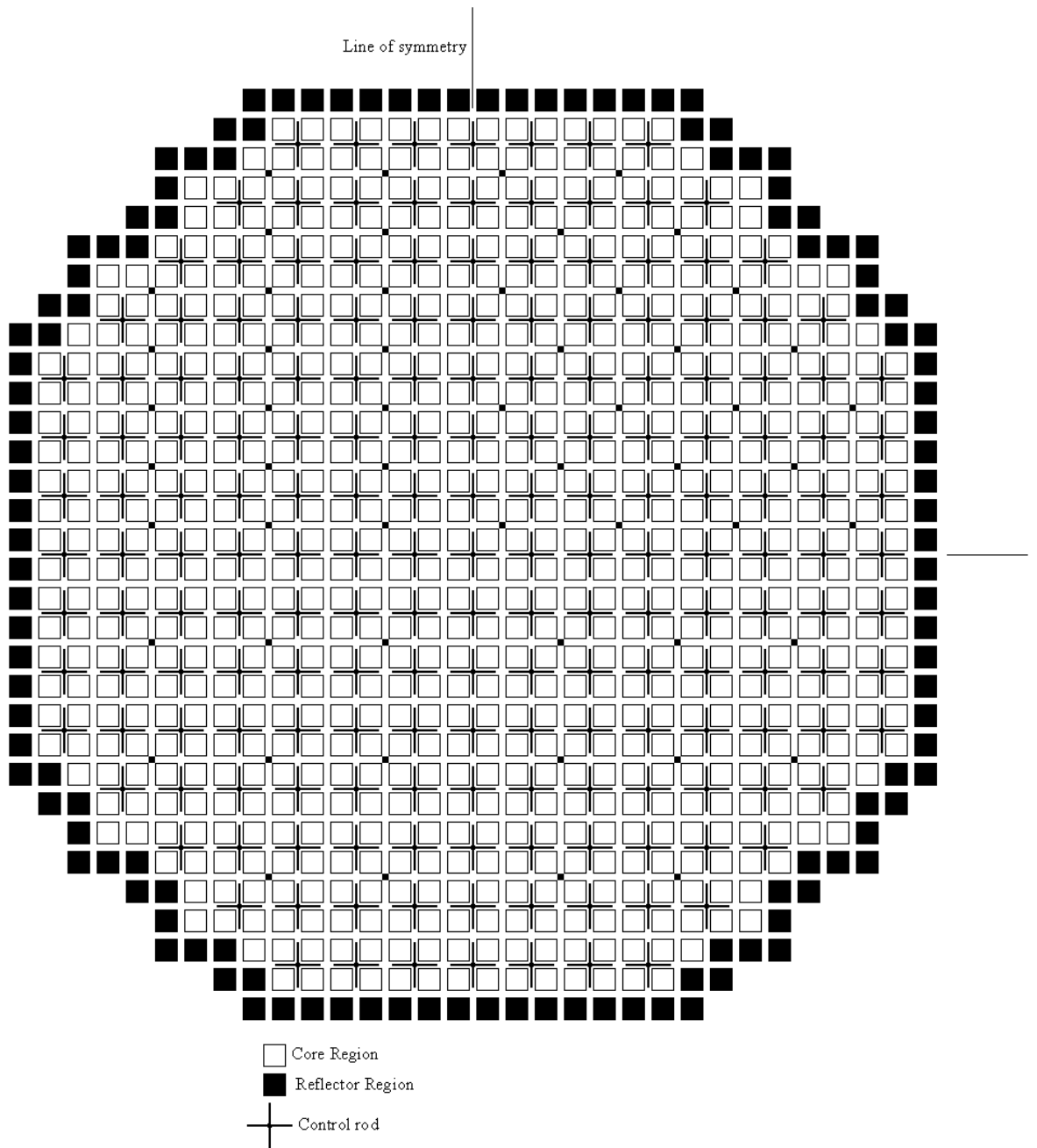
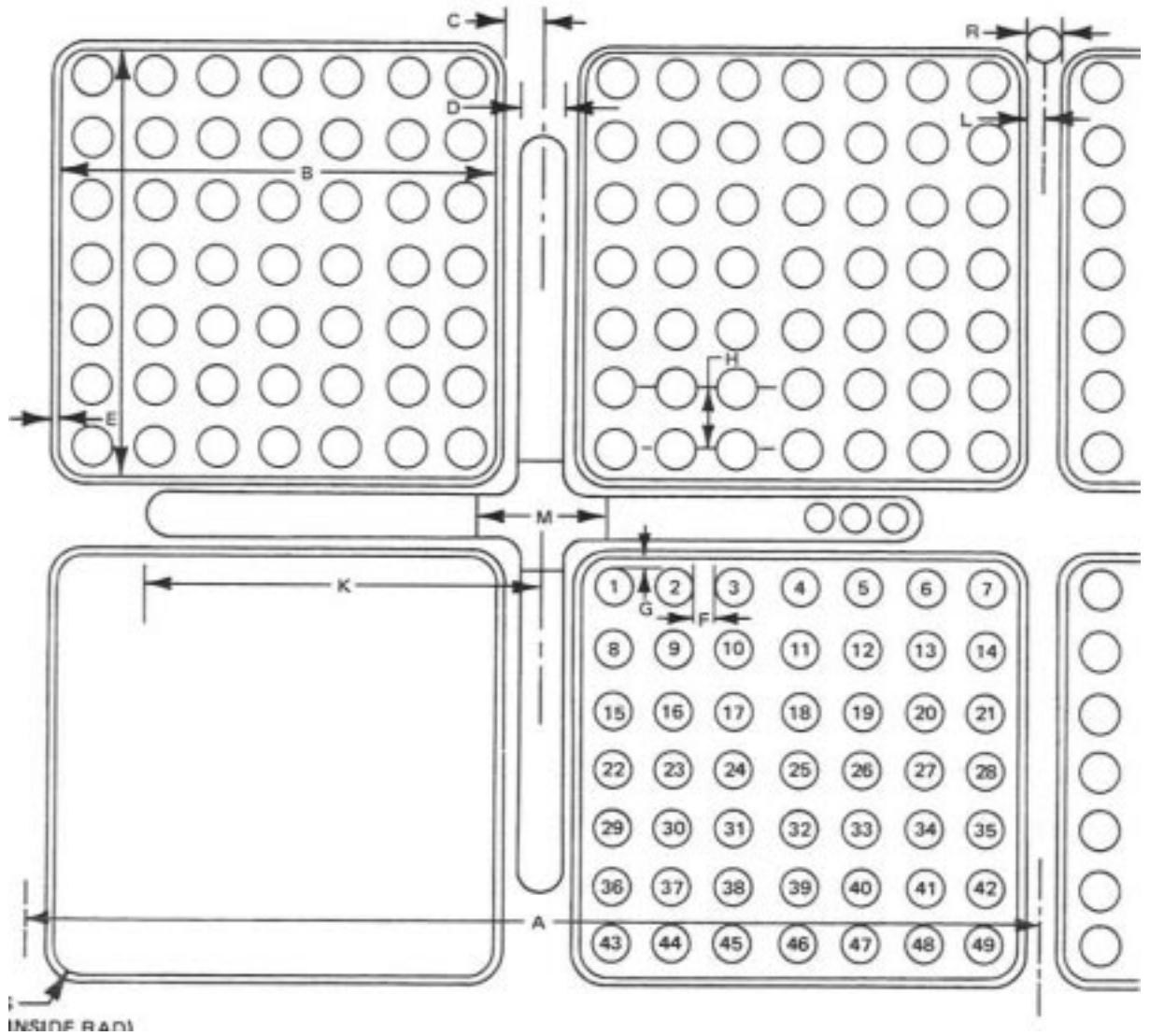
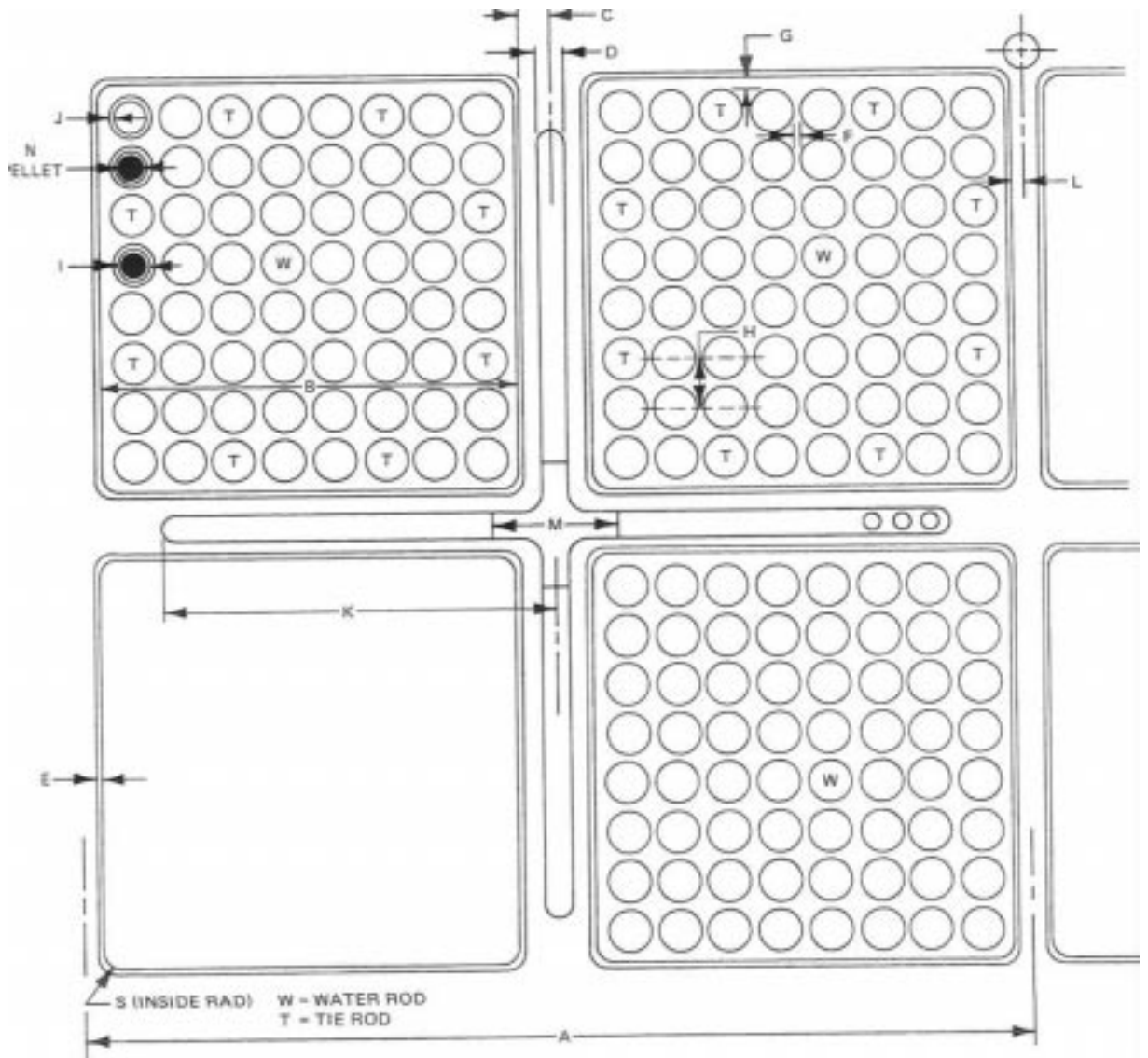


Figure 2.2.2 PB2 initial fuel assembly lattice



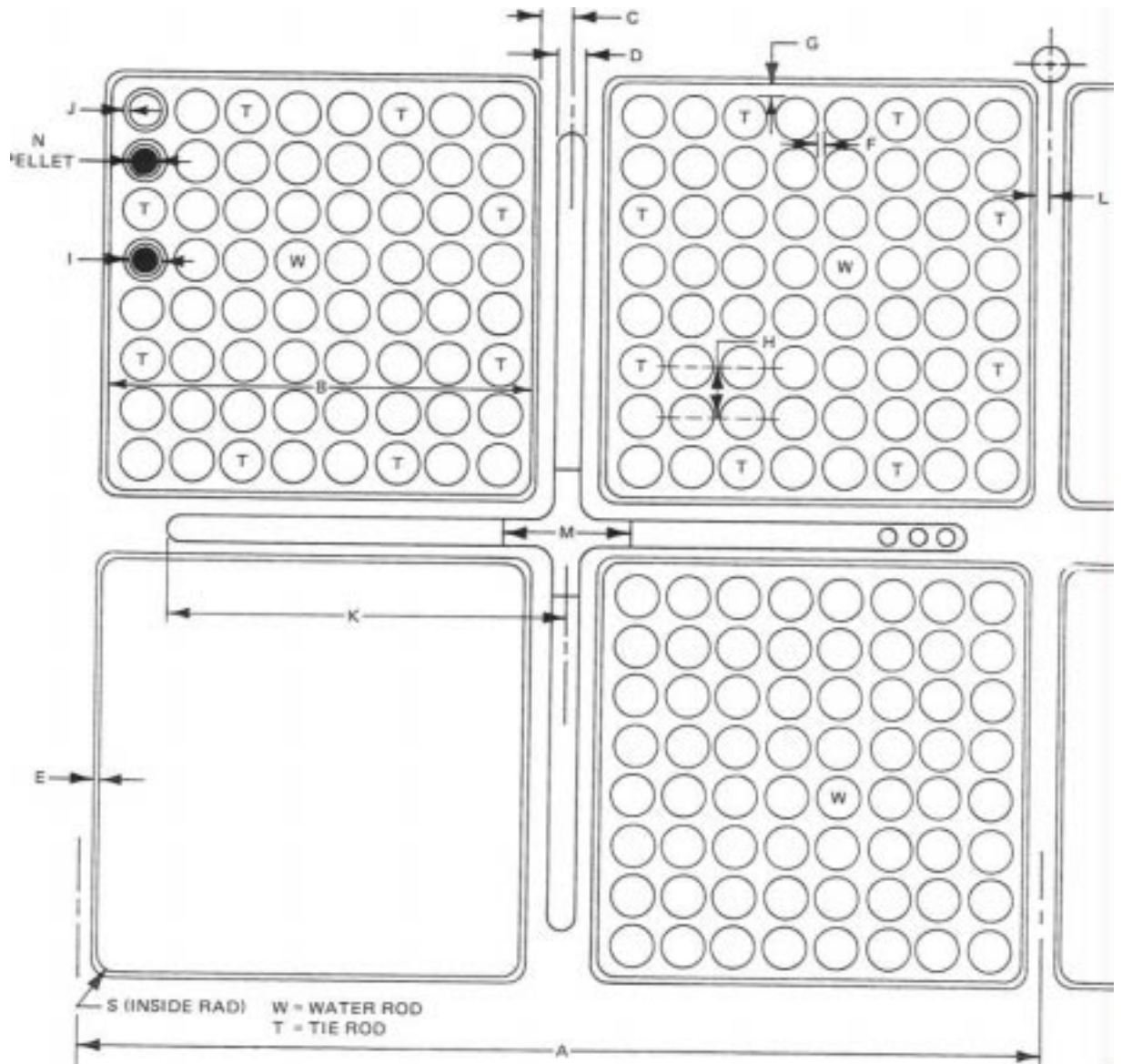
DIM. ID.	A	B	C	D	E	F	G	H	I	J
DIM. Inches	12.0	5.278	0.375		0.080	0.175	0.1435	0.738		
DIM cm	30.48	13.40612	.9525		.2032	.4445	.36449	1.87452		
DIM. ID.	K	L	M	N	O	P	Q	R	S	
DIM. Inches		0.187							0.38	
DIM. cm		.47498							.9652	

Figure 2.2.3 PB2 reload fuel assembly lattice for 100 mil channels



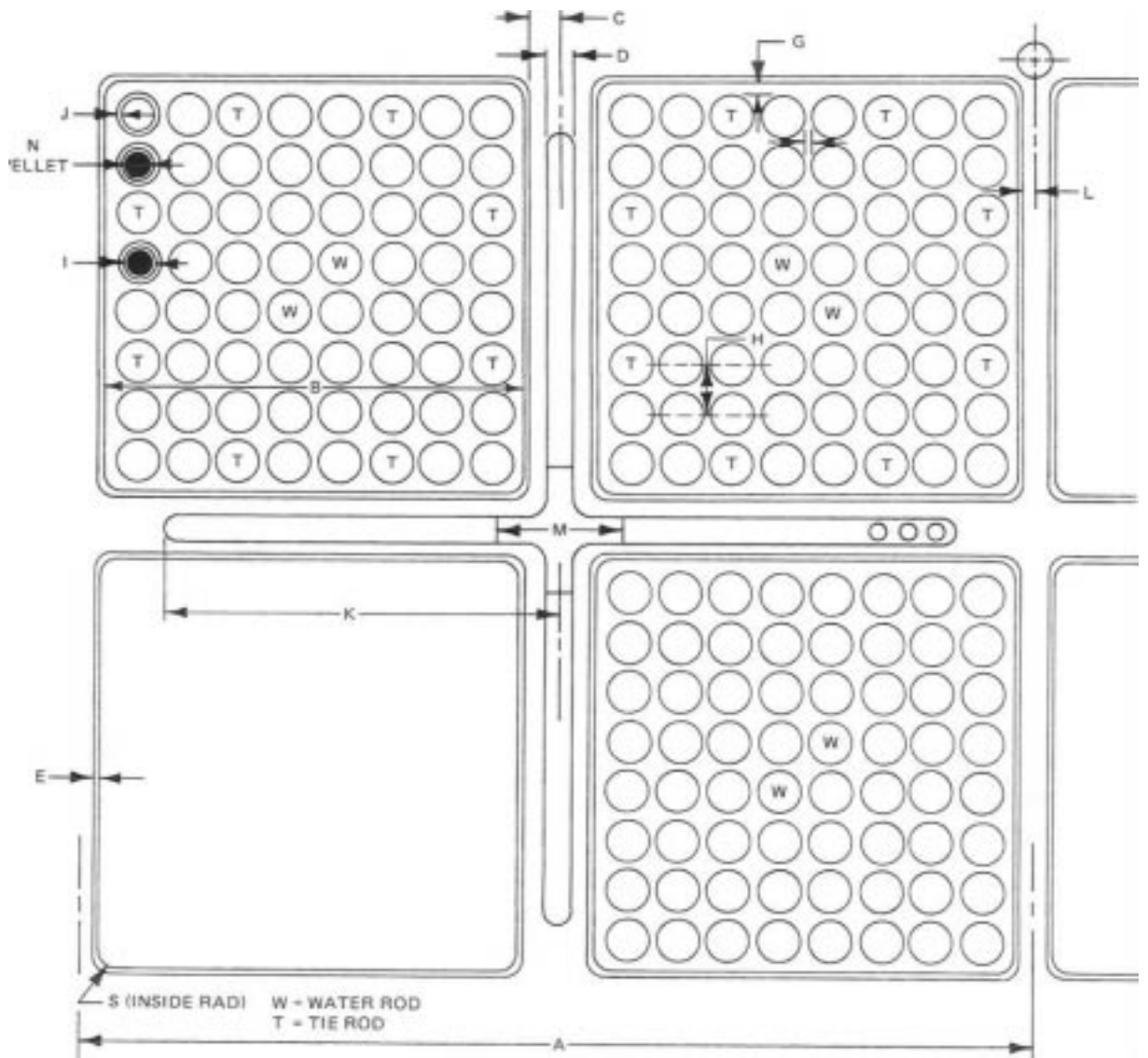
DIM. ID.	A	B	C	D	E	F	G	H	I	J
DIM. Inches	12.0	5.278	0.355		0.100	0.147	0.153	0.64		
DIM cm	30.48	13.4061 2	.9017		.254	.37338	.38862	1.6256		
DIM. ID.	K	L	M	N	O	P	Q	R	S	
DIM. Inches		0.167							0.38	
DIM. cm		.42418							.9652	

Figure 2.2.4 PB2 reload fuel assembly lattice for 120 mil channels



DIM. ID.	A	B	C	D	E	F	G	H	I	J
DIM. Inches	12.0	5.278	0.33 5		0.120	0.147	0.153	0.64		
DIM cm	30.48	13.4061 2	.850 9		.3048	.3733 8	.38862	1.625 6		
DIM. ID.	K	L	M	N	O	P	Q	R	S	
DIM. Inches		0.147							0.38	
DIM. cm		.42418							.9652	

Figure 2.2.5 PB2 reload fuel assembly lattice for LTA assemblies



DIM. ID.	A	B	C	D	E	F	G	H	I	J
DIM. Inches	12.0	5.278	0.355		0.100	0.157	0.158	0.64		
DIM cm	30.48	13.40612	.9017		.254	.39878	.40132	1.6256		
DIM. ID.	K	L	M	N	O	P	Q	R	S	
DIM. Inches		0.167							0.38	
DIM. cm		.42418							.9652	

Figure 2.4.2 Radial Distribution of Assembly Types

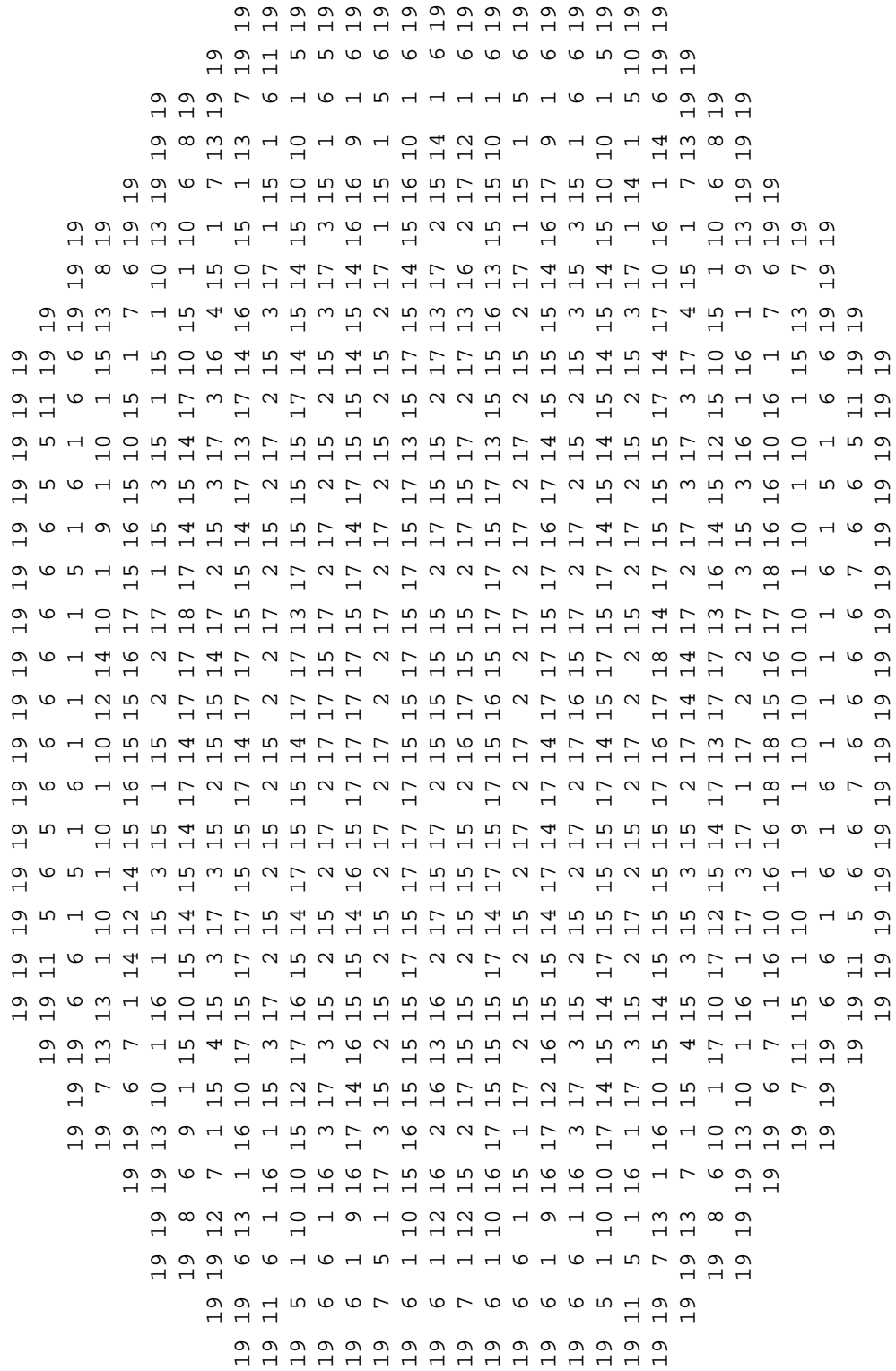


Figure 2.5.1 Fuel assembly orientation for ADF assignment

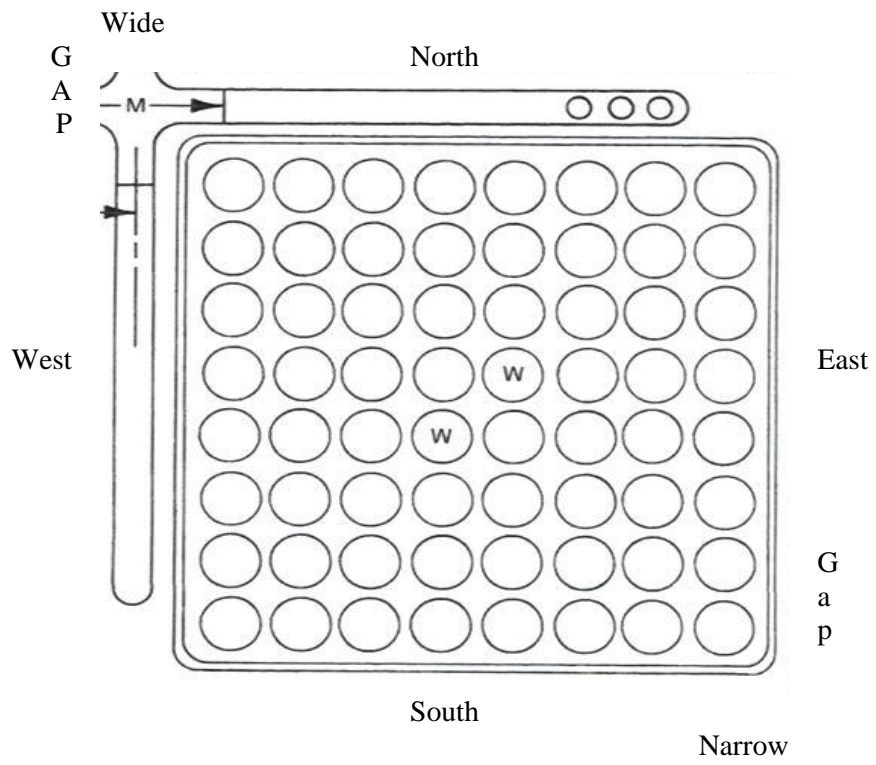


Figure 2.6.1. Core orificing and TIP system arrangement

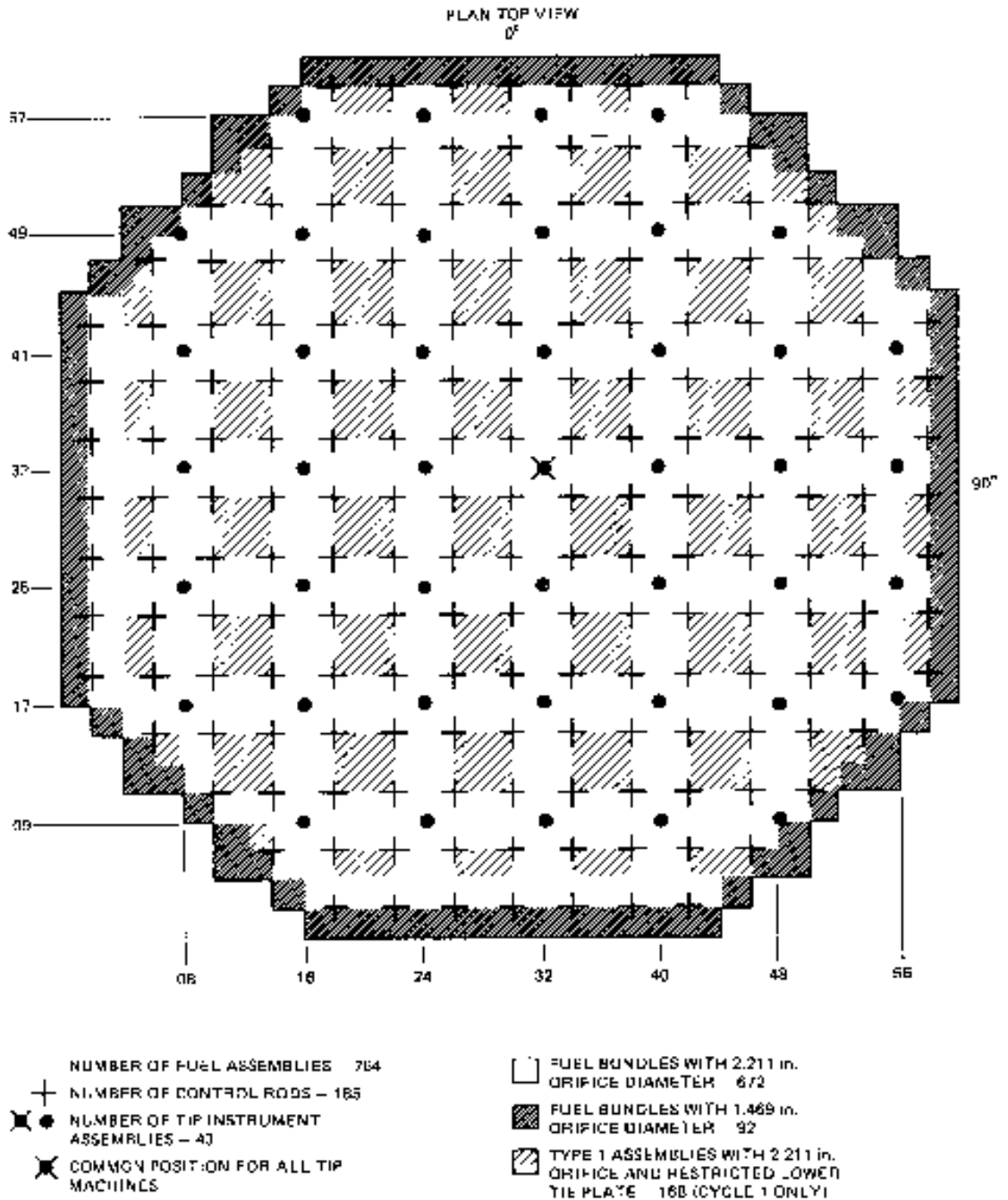
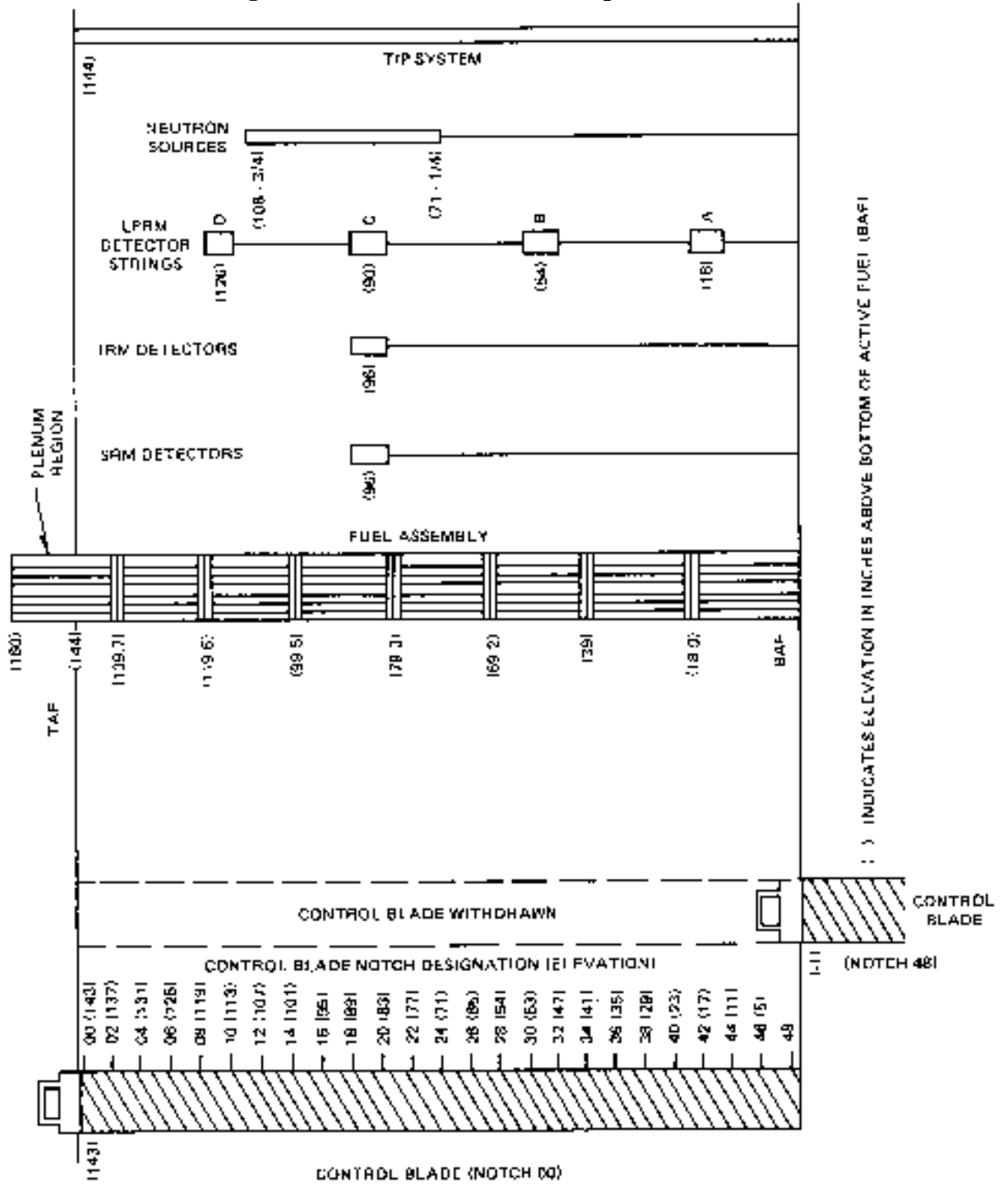


Figure 2.6.2. Elevation of core components



Chapter 3

Thermal-hydraulic data

A PB2 RETRAN [4] thermal-hydraulic skeleton input deck, as well as the PB2 RETRAN model nodalization and steam line nodalization diagrams, are provided in Appendix A. English units are used in this skeleton deck (e.g., ft, ft², etc.). The detailed plant drawings are provided in Ref. [2].

3.1 Component specifications for the full thermal-hydraulic system model

3.1.1. Reactor vessel

The following tables provide all of the necessary data about the PB2 Reactor Vessel. Table 3.1.1.1 contains the design data, and Table 3.1.1.2 contains the volume data. Table 3.1.1.3 contains important PB2 reference design information. Please note that the volumes and elevations in the skeleton input deck, given in Appendix A, are based on the nodalization used for that deck as shown in Figure 3.1.1.1. These volumes and elevations involve combining different physical regions together. In contrast, the values given in the tables are the actual physical volumetric data obtained from the actual vessel dimensions. See Figure 3.1.1.1 for the way in which the core regions are defined in the RETRAN skeleton input deck. Figure 3.1.1.1 also shows the flow paths of the reactor vessel, reactor recirculation system, and steam lines. As it can be seen in Figure 3.1.1.1, a single volume (volume 7) is used to model the steam space above the steam separators. The down comer region is divided into three volumes. The upper downcomer (volume 8) models the region surrounding the steam separators and includes the normal steam-water interface. The middle downcomer (volume 9) models the region surrounding the standpipes and is the volume where the feedwater flow and the liquid flow from the steam separators mixes. The lower downcomer models the region surrounding the core shroud and jet pumps. Flow to the recirculation loops and jet pump suctions are from this volume.

A single volume (volume 1) is used to model the fluid region below the core support plate (lower plenum). The upper plenum region above the upper guide plate and the standpipes are both modeled as single volumes (volume 4 and 5). Two-sided, passive heat conductors are used to model the material of the shroud head and the standpipes. A single volume is used to model the internal volume of the 211 steam separators. Since the liquid flow from the separators, which includes any steam carryunder, enters the subcooled middle downcomer, the effects of carry-under can be ascertained without introducing steam bubbles into the liquid downcomer.

3.1.2 Reactor recirculation system

This section provides the participants with the data for the reactor recirculation system (RRS). Table 3.1.2.1 summarizes the basic RRS parameters. The two recirculation loops are modeled separately. Each recirculation loop is modeled with three fluid volumes: suction, pump, and discharge (volumes 11, 12, 13, 14, 15, and 16). Each loop drives ten jet pumps lumped as one.

Actual pump data is used to input pump performance parameters in the normal operating quadrants based on built-in curves for a pump of similar specific speed. Rated values for pump flow, head, and torque are based on actual pump data, as is the pump moment of inertia.

The included jet pump model corresponds to the simplified TRAC-BF1 JETP component model. The main features and geometric characteristics of the jet pump are captured in this model and it is shown in Figure 3.1.2.1. Table 3.1.2.2 provides the geometric characteristics. To better understand how the model is built, Figure 3.1.2.1 along with Table 3.1.2.2 should be used. Note that the information provided in Table 3.1.2.2 corresponds to a single jet pump. For the participants whose codes do not include a jet-pump model capability, a write-up containing a jet-pump model can be found on the benchmark side under the Specifications directory. The name of the file is jet-pump.doc.

3.1.3 Core region

Twenty-four fluid volumes (volumes 101-124) are used to model the active (i.e., fueled) region of the core. Additionally, single volumes are used to model an unheated core inlet region and core outlet region (volumes 2 and 125). The entire core bypass region is modelled with one fluid volume (volume 3)

Loss coefficients for the central and peripheral core inlet orifice are provided in Table 3.1.3.1. Table 3.1.3.2 presents the fuel region loss coefficients for each the fuel types present in the PB2 reactor core at end cycle (EOC) 2. Table 3.1.3.3 provides hydraulic leakage characteristics for the 7x7 and 8x8 fuel designs.

3.1.4 Steam lines

The four main steam lines are lumped into one line, which is divided into six volumes (volumes 50, 51, 52, 53, 54, and 55). Two of the volumes (50 and 51) model the steam lines inboard of the main steam isolation valves (MSIVs). The second inboard volume is connected to the junctions representing the safety/relief valves (SRVs). Table 3.1.4.1 summarizes the safety relief valves reference design information. Note that no safety/relief valves are actuated during the actual TT2 test. The remaining four volumes (volumes 52, 53, 54, and 55) model the steam lines from the MSIVs to the turbine stop/control valves.

The steam bypass system is modelled up to and including the condenser (volumes 200, 201, 202, and 500). The condenser is modelled as a boundary condition. Important junctions parameters such as flow areas and flow pressure loss coefficients are based on steam bypass system design data. Steam bypass system reference design data is provided in Table 3.1.4.2.

3.1.5 Feedwater lines

The feedwater lines are not modeled as fluid volumes. Instead, a fill junction is used to specify the feedwater mass flow as a boundary condition. Time-dependent feedwater flow is provided later in Chapter 5 (Table 5.3.3).

3.2 Definition of the core thermal-hydraulic boundary conditions model

The PB2 thermal-hydraulic model can be converted to a core thermal-hydraulic boundary condition model by defining inlet and outlet thermal-hydraulic boundary conditions. The

developed model for performing the 3-D core thermal-hydraulic boundary condition calculation (Option 1 of Exercise 2) was built based on different TRAC-BF1 thermal-hydraulic components as follows. A 33-channel thermal-hydraulic core boundary condition model was obtained from the PB2 TT2 TRAC-BF1 system model. Bottom and top boundary conditions are specified in this model using the FILL and BREAK TRAC-BF1 components. The developed model is illustrated in Figure 3.2.1. Figure 3.2.2 shows the thermal-hydraulic radial mapping scheme used to represent PB2 reactor core. The 33 thermal-hydraulic channels shown on this figure are coupled to the neutronic code model in the radial plane as it was shown in Figure 2.4.1 of Chapter 2. Thermal-hydraulic channels identified with zeroes are treated as reflector regions. This mapping scheme follows the spatial mesh overlays developed for the PB2 TRAC-BF1/NEM 3D neutron kinetics/thermal-hydraulic model. The core boundary condition model using 1-D kinetics (Option 2 of Exercise 2) could use the system thermal-hydraulic model developed for Exercise 1 and 3 or just use one average channel for representing the whole core plus the bypass channel.

There are several files of data available at the ftp site and on the CD-ROM that are used for definition of the core thermal-hydraulic boundary condition model. This data is taken from a combination of the best-estimate core plant system code calculations performed and test data. The Boundary conditions provided to the participants are both steady state and time dependent. They are provided for the bottom and top regions adjacent to the inlet and outlet region of the core region. These values are obtained from the lower and upper region of the vessel component of the TRAC-BF1 model. The types of boundary conditions that are provided to the participants are:

1. At the inlet of the channels: mass flows (kg/s) and temperatures (K) from 0 s to 5 s. 33 files are provided since the model used to obtain these variables contains 33 thermal-hydraulic channels. In addition a single file that contains core mass flow and core inlet temperature vs. time is provided to the participants whose thermal-hydraulic models consist of a single average channel.
2. At the outlet of the thermal-hydraulic channels: pressure (Pa) from 0 s to 5 s. Since all the channels have a common plenum, pressure is constant radially. Therefore a single file, containing pressure vs. time information is provided.

3.3 Thermal-physical and heat transfer specifications

3.3.1 Nuclear fuel (UO₂-PuO₂) properties

Doppler Temperature

The average fuel temperature is used for feedback purposes. This value should be obtained from the fuel rod model of each code.

Density

$$\rho = f_{TD} \left[(1 - f_{PuO_2}) \rho_{UO_2} + f_{PuO_2} \rho_{PuO_2} \right]$$

where

f_{TD} = fraction of theoretical density (0.95)

f_{PuO_2} = weight fraction of PuO₂ in fuel (default = 0.0)

$$\rho_{\text{UO}_2} = 1.097\text{E}4 \text{ kg/m}^3$$

$$\rho_{\text{PuO}_2} = 1.146\text{E}4 \text{ kg/m}^3$$

Specific Heat

$$C_p = 15.496 \left[\frac{b_1 b_4^2 \exp\left(\frac{b_4}{T}\right)}{T^2 \left[\exp\left(\frac{b_4}{T}\right) - 1 \right]^2} + 2b_2 T + \frac{b_3 b_5}{b_6 T^2} \exp\left(\frac{-b_5}{b_6 T}\right) \right]$$

where

$$\begin{aligned} C_p &= \text{specific heat capacity (J/kgK)} \\ T &= \text{fuel temperature (K)} \\ b_1 &= 19.145 \text{ for UO}_2; 19.53 \text{ for UO}_2\text{-PuO}_2 \\ b_2 &= 7.8473\text{E}^{-04} \text{ for UO}_2; 9.25\text{E}^{-04} \text{ for UO}_2\text{-PuO}_2 \\ b_3 &= 5.6437\text{E}^{+06} \text{ for UO}_2; 6.02\text{E}^{+06} \text{ for UO}_2\text{-PuO}_2 \\ b_4 &= 535.285 \text{ for UO}_2; 539.0 \text{ for UO}_2\text{-PuO}_2 \\ b_5 &= 37694.6 \text{ for UO}_2; 40100.0 \text{ for UO}_2\text{-PuO}_2 \\ b_6 &= 1.987 \text{ for UO}_2; 1.987 \text{ for UO}_2\text{-PuO}_2 \end{aligned}$$

Thermal Conductivity

For $T_c < T_1$

$$k = c \left[\frac{c_1}{c_2 + T_c} + c_3 \exp(c_4 T_c) \right] \text{ in W/m-K}$$

for $T_c > T$

$$k = c [c_5 + c_3 \exp(c_4 T_c)] \text{ in W/m-K}$$

where

$$\begin{aligned} T_c &= \text{temperature (}^\circ\text{C)} \\ f_{\text{TD}} &= \text{fraction of theoretical density} \end{aligned}$$

$$c = 100.0 \left[\frac{1 - \beta(1 - f_{\text{TD}})}{1 - 0.05\beta} \right] = 100.0, \text{ for } f_{\text{TD}} = 0.95$$

$$\beta = c_6 + c_7 T_c$$

and

$$c_1 = 40.4 \text{ for UO}_2; 33.3 \text{ for UO}_2\text{-PuO}_2$$

c_2	=	464.0 for UO_2 ; 375.0 for $\text{UO}_2\text{-PuO}_2$
c_3	=	1.216E^{-04} for UO_2 ; 1.54E^{-04} for $\text{UO}_2\text{-PuO}_2$
c_4	=	1.867E^{-03} for UO_2 ; 1.71E^{-03} for $\text{UO}_2\text{-PuO}_2$
c_5	=	0.0191 for UO_2 ; 0.0171 for $\text{UO}_2\text{-PuO}_2$
c_6	=	2.58 for UO_2 ; 1.43 for $\text{UO}_2\text{-PuO}_2$
c_7	=	-5.8E^{-04} for UO_2 ; 0.0 for $\text{UO}_2\text{-PuO}_2$
T_1	=	1650.0 for UO_2 ; 1550.0 for $\text{UO}_2\text{-PuO}_2$

3.3.2 Gas gap conductance

All participants should use the following constant value:

$$K_{\text{gap}} = 4542.56 \frac{\text{W}}{\text{m}^2 - \text{K}} \left(800 \frac{\text{BTU}}{\text{hr} - \text{ft}^2 - \text{F}} \right)$$

3.3.3 Zircaloy cladding properties

Density

A constant value is used;

$$\rho = 6551.4 \text{ kg/m}^3$$

Specific Heat

For $T > 1248 \text{ K}$, $C_p = 356 \text{ J/kgK}$

For $T \leq 1248 \text{ K}$, use Table 3.3.3.1

Thermal Conductivity

The following expression is used to calculate cladding thermal conductivity;

$$k = a_0 + a_1 T + a_2 T^2 + a_3 T^3$$

where

k	=	thermal conductivity (W/m-K)
T	=	temperature (K)
a_0	=	7.51 for Zr, 1.96 for ZrO_2
a_1	=	2.09E^{-02} for Zr, -2.41E^{-04} for ZrO_2
a_2	=	-1.45E^{-05} for Zr, 6.43E^{-07} for ZrO_2
a_3	=	7.67E^{-09} for Zr, -1.95E^{-10} for ZrO_2

Expansion effects of fuel and cladding will not be considered in this benchmark. The heat transfer coefficient between cladding and moderator, as well as heat transfer across the pellet-clad gap, has to be calculated using code specific correlations.

Table 3.1.1.1 Reactor vessel design data

Item	Data
Reactor Vessel	
Operating temperature (°F/°K)	575/574.82
Inside length (in/m)	875.125/22.228
Design Pressure (psig/Pa)	1250/8719771
Vessel Nozzles (number - size, in/cm)	
Recirculation outlet	2 - 28/71.12
Steam Outlet	4 - 26/66.04
Recirculation inlet	10 - 12/30.48
Feedwater inlet	6 - 12/30.48
Core spray inlet	2 - 10/25.4
Instrument (one of these is head spray)	2 - 6/15.24
CRD	185 - 6/15.24
Jet pump instrumentation	2 - 4/10.16
Vent	1 - 4/10.16
Instrumentation	2 - 6/15.24
CRD hydraulic system return	1 - 4/10.16
Core differential pressure and liquid control	1 - 2/5.08
Drain	1 - 2/5.08
In-core flux instrumentation	55 - 2/5.08
Head seal leak detection	2 - 1/2.54
Weights (lb/kg)	
Bottom head	207500/94120.4
Vessel shell	842300/382061
Vessel flange	105800/47990.1
Support skirt	28200/12791
Other vessel components	65000/29484
Total Vessel without top head	1248800/566446.2
Top head	252200/114396
Total vessel	1501000/680842.1

Table 3.1.1.2 Peach Bottom-2 Vessel fluid volumes

Height Above Vessel Bottom (in/m)	Vessel Fluid Volume (in ³ /m ³)
50.98/1.295	1.2635E06/20.705
125.5/3.188 ¹	4.2975E06/75.425
191.1/4.855 ²	6.43282E06/105.415
216.2/5.494 ²	7.08602E06/116.119
360.3/9.152 ²	1.01257E07/165.931
379.1/9.630 ²	1.05203E07/172.396
411.61/10.455 ²	1.16880E07/191.532
442.64/11.243 ²	1.24879E07/204.640
442.64/11.243 ³	1.73009E07/283.511
562.52/14.288 ⁴	2.31777E07/379.814
587.01/14.910 ⁵	2.36546E07/387.629
635.00/16.129 ⁶	2.64199E07/432.945
739.02/18.771	3.15989E07/517.813
870.51/22.111	3.57389E07/585.655
<p>1 Include volume of jet pumps</p> <p>2 Inside shroud vessel only</p> <p>3 Include volume outside of shroud vessel</p> <p>4 Include steam separator returning water volume</p> <p>5 Does not include steam volume leaving steam separators</p> <p>6 Include steal volume leaving steam separators</p>	

Table 3.1.1.3 PB2 Reference design information

Parameter	Value
Rated core thermal power, MWt	3293
Rated core total flow rate, (Mlb/hr)/(kg/s)	102.5/12915
Bypass flow rate, fraction of total core flow	Ref. [2], Figs. 54-55
Fraction of core thermal power passing through fuel cladding	.96
Approximate bypass coolant total power fraction	.02
Approximate active coolant total power fraction	.02
Approximate channel wall direct heating fraction	.0075
Design minimum critical power ratio for 7x7 assemblies (Cycle 2)	≥1.28
Design minimum critical power ratio for 8x8 assemblies (Cycle 2)	≥1.31
Design overpower for turbine-generator system	105% rated steam
Turbine inlet pressure, psia/Pa	965/6.653E06
Rated reactor dome pressure, psia/Pa	1020/7.033E06
Rated steam flow rate, (Mlb/hr)/(kg/s)	13.381/1685.98
Steam moisture content, fraction	.001
Rate steam dryer and separator pressure drop, psia/Pa	15/103421
Rated core pressure, psia/Pa	1035/7.1361E06
Core pressure drop at rated conditions, psia/Pa	22/151685
Approximate core inlet pressure, psia/Pa	1060/7.3084E06
Core inlet enthalpy, (Btu/lb)/(J/kg)	521.3/1.2125E06
Enthalpy rise across core, (Btu/lb)/(J/kg) (average)	109.6/2.5491E05
Core support plate pressure drop, psi/Pa	18/1.24105E05
Core orifice and lower tie plate pressure drop, Pa	Ref. [2], Figs. 48-53
Fuel bundle pressure drop	Ref. [2], Figs. 44-47
Reactor average exit quality at rated conditions	.129
Design hot channel active coolant exit quality	.25
Design bypass coolant exit quality	.0
Total feedwater flow rate, (Mlb/hr)/(kg/s)	13.331/1679.7
Feedwater temperature, °F/°K	376.1/464.32
Control rod drive flow rate, (lb/hr)/(kg/s)	50000/6.2999
Control rod drive flow temperature, °F/°K	80/299.82
Cleanup demineralizer flow rate, (lb/hr)/(kg/s)	133300/16.7958
Cleanup demineralizer inlet temperature, °F/°K	528/548.7
Cleanup demineralizer outlet temperature, °F/°K	431/494.82
Location of demineralized water return	Feedwater line
Jet pump design M ratio	1.96
Jet pump design N ratio	.16
Number of recirculation pumps	2
Recirculation pump type	Centrifugal
Recirculation pump rated flow, (Mlb/hr)/(kg/s)	17.1/2154.56
Total developed pump head, ft/m	710/216.41
Recirculation pump efficiency, percent	87
Head loss from vessel recirculation outlet to vessel inlet, ft/m	59/17.98
Head loss from vessel recirculation inlet to jet pump 180° bend entrance, ft/m	11/3.353

Table 3.1.2.1 Reactor recirculation system design characteristics

Item	Data
External loops	
Number of loops	2
Pipe sizes (nominal O.D.)	
Pump suction, in/cm	28/71.12
Pump discharge, in/cm	28/72.12
Discharge manifold, in/cm	22/55.88
Recirculation inlet line, in/cm	12/30.48
Cross-tie line, in/cm	22/55.88
Design pressure (psig/Pa), design temperature (°F/°K)	
Suction piping	1148/8016506, 562/567.59
Discharge piping	1326/9243773, 562/567.59
Pumps	1500/1.044346E07, 575/574.82
Operation at rated conditions	
Recirculation pump	
Flow gpm/(m ³ /s) (approximate)	45200/2.851677
Flow, (lb/hr)/(kg/s)	1.71E07/2154.56
Total developed head, ft/m	710/216.408
Suction pressure (static), psia/Pa	1032/7115389
Available NPSH* (min.), hp/W	500/373000
Water temperature (max.), °F/°K	528/548.71
Pump hydraulic HP (min.), hp/W	6130/4572980
Flow velocity at pump suction, fps/(m/s) (approximate)	27.5/8.382
Drive motor and power supply	
Frequency (at rated), Hz	56
Frequency (operating range), Hz	11.5-57.5
Total required power to M-G sets	
KW/set	6730
KW/total	13460
Jet pumps	
Number	20
Total jet pump flow, (lb/h)/(kg/s)	1.025E08/12915
Throat I.D., in/cm	8.18/20.7772
Diffuser I.D., in/cm	19.0/48.26
Nozzle I.D., in/cm (representative)	3.14/7.9756
Differ exit velocity, fps/(m/s)	15.3/4.6634
Jet pump head, ft/m	76.1/23.195

Table 3.1.2.2 PB2 BWR TRAC-BF1 simplified jet pump model

Primary Tube (four thermal-hydraulic cells)	
Inner radius of the primary tube wall, m	0.14009
Wall thickness of the primary tube wall, m	0.00635
Cell lengths, m	2.5766, 0.30531, 1.8865, 0.24232
Cell volumes, m ³	0.091159, 0.013037, 0.20718, 0.044325
Cell edge flow areas, m ²	0.070412, 0.03538, 0.050468, 0.018292, 0.018292
Hydraulic diameters, m	0.2286, 0.21224, 0.25349, 0.4826, 0.4826
Side Tube (2 thermal-hydraulic cells)	
Inner radius of the side tube wall, m	0.080772
Wall thickness of the side tube wall, m	0.00635
Cell lengths, m	0.39675, 0.41893
Cell volumes, m ³	0.007811, 0.01275
Cell edge flow areas, m ²	0.0052537, 0.030434, 0.030434
Hydraulic diameters, m	0.081788, 0.19685, 0.19685,

Table 3.1.3.1 Core related hydraulic loss coefficients (inlet orifices)
(K/A²)

Central core inlet orifice, in ⁻⁴ /cm ⁻⁴	0.1293/0.003106
Peripheral core inlet orifice, in ⁻⁴ /cm ⁻⁴	0.7916/0.01902

Table 3.1.3.2 Fuel estimated loss coefficients
(K/A²)

	7x7 Fuel type	8x8 Fuel type
Fuel lower tie plate, in ⁻⁴ /cm ⁻⁴	0.0320/0.000769	0.0344/0.000826
Fuel spacers, in ⁻⁴ /cm ⁻⁴	0.00450/0.000108	0.00502/0.000121
Fuel upper tie plate, in ⁻⁴ /cm ⁻⁴	0.00490/0.000118	0.00510/0.000123

Table 3.1.3.3 Core related hydraulic leakage flows	
7x7 Bundle Leakage (central, per assembly), lbm/hr/kg/s	4600/0.5796
7x7 Bundle Leakage (peripheral, per assembly), lbm/hr/kg/s	1150/0.1449
8x8 Bundle Leakage (central, per assembly), lbm/hr/kg/s	10860/1.36836
8x8 Water Rod (central, per assembly) , lbm/hr/kg/s	920/0.11592
Core Plate Leakage, Mlbm/hr/kg/s	2.14/269.64
Total Leakage, Mlbm/hr/kg/s	6.68/841.68

Table 3.1.4.1 Nuclear system safety and relief valves

	Number of Valves	Set pressure, (psig/Pa)	Capacity at 103% of set pressure (each), (lb/h)/(kg/s)
Relief valves	4	1105/7.720E06	819000/103.19
	4	1115/7.789E06	827000/104.20
	3	1125/7.858E06	834000/105.08
Total**	11(5)		
Safety valves	2	1230/8.582E06	

** The number in parentheses indicates the number of relief valves, which serve in the automatic depressurisation capacity.

Table 3.1.4.2 Steam bypass design data

Number of valves	9
Design flow (per valve), lbm/hr/kg/s	390000/49.13
Design inlet pressure, psia/Pa	965/6653675
Design outlet pressure (downstream of valves, psia/Pa)	724/4991980
Pressure at entrance to condenser, psia/Pa	250/1723750

Table 3.3.3.1 Specific heat of Zircaloy versus Temperature for $T \leq 1248$ K

T (K)	C_p (J/kgK)
300	281
400	302
640	331
1090	375
1093	502
1113	590
1133	615
1153	719
1173	816
1193	770
1213	619
1233	469
1248	356

Figure 3.1.1.1 PB2 RETRAN Thermal-Hydraulic Model

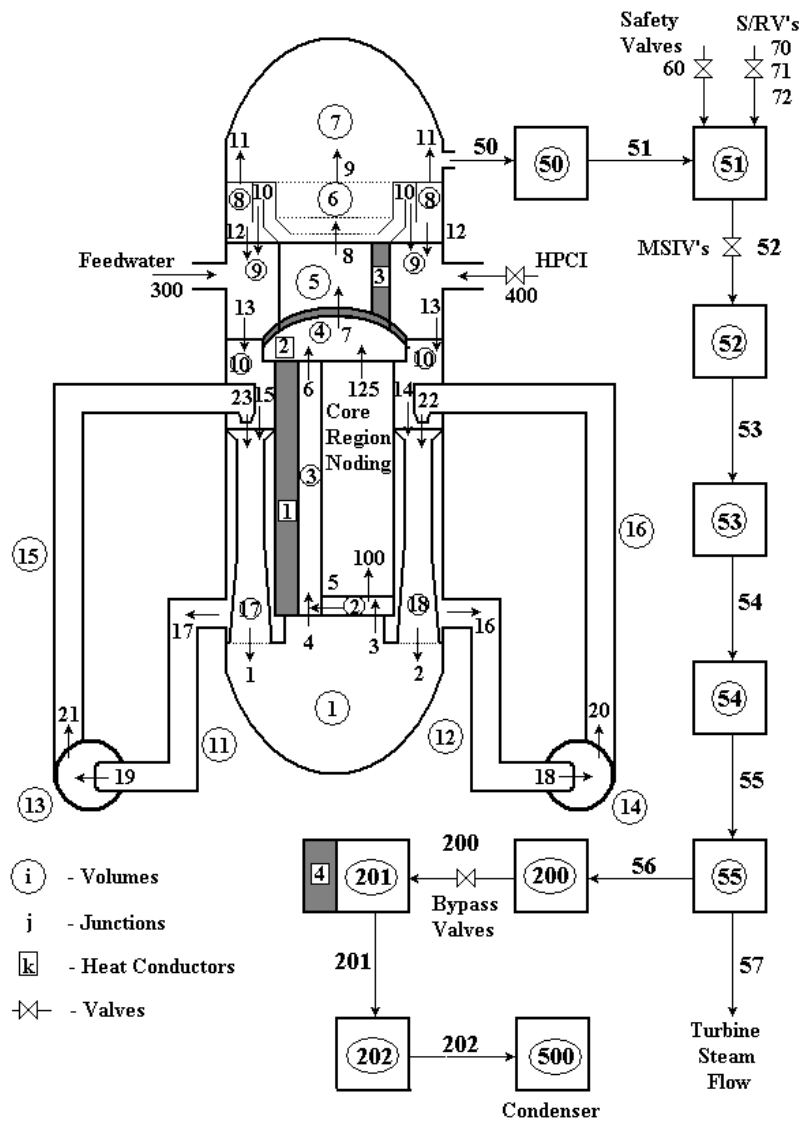


Figure 3.1.2.1 Simplified TRAC-BF1 BWR jet pump model

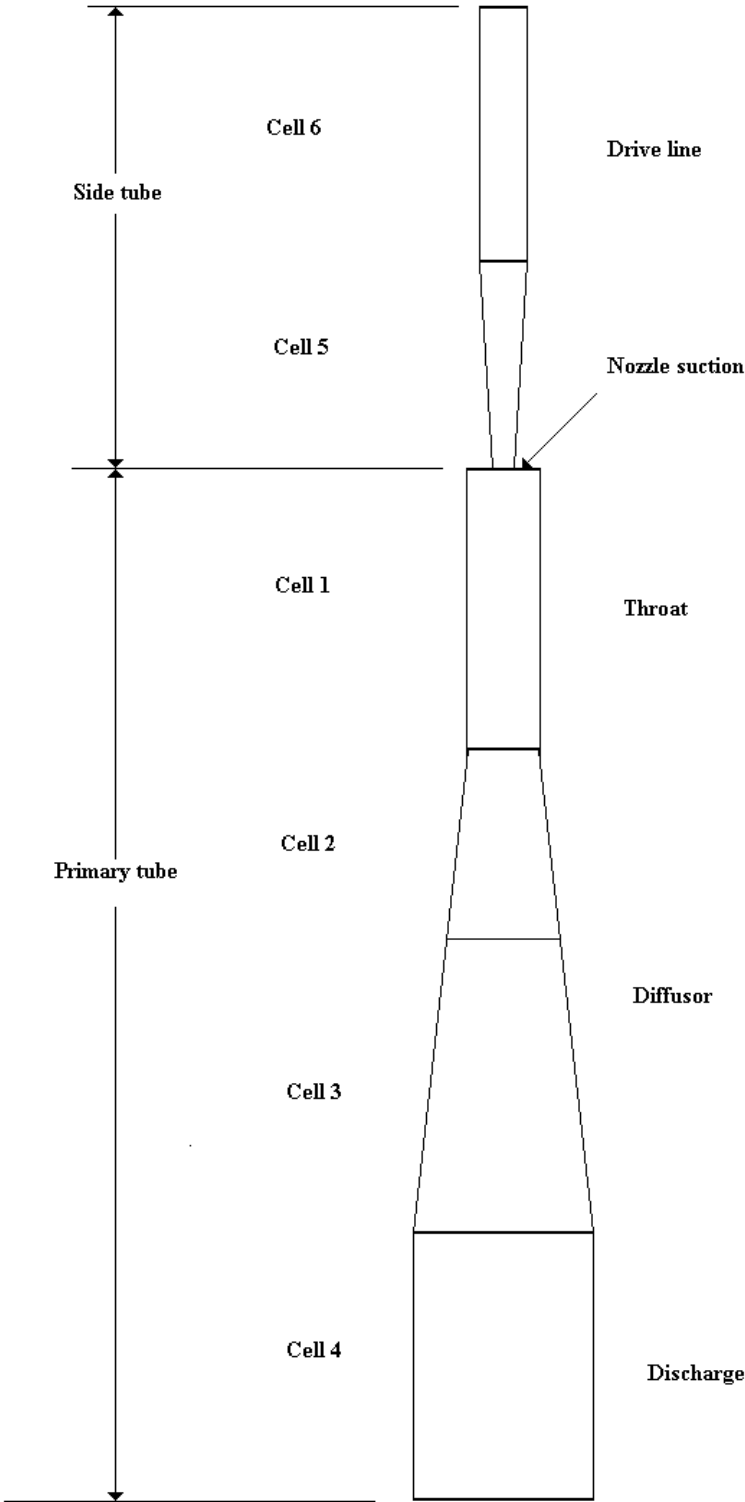


Figure 3.2.1 PB2 OECD/NRC TT vessel/core boundary conditions model

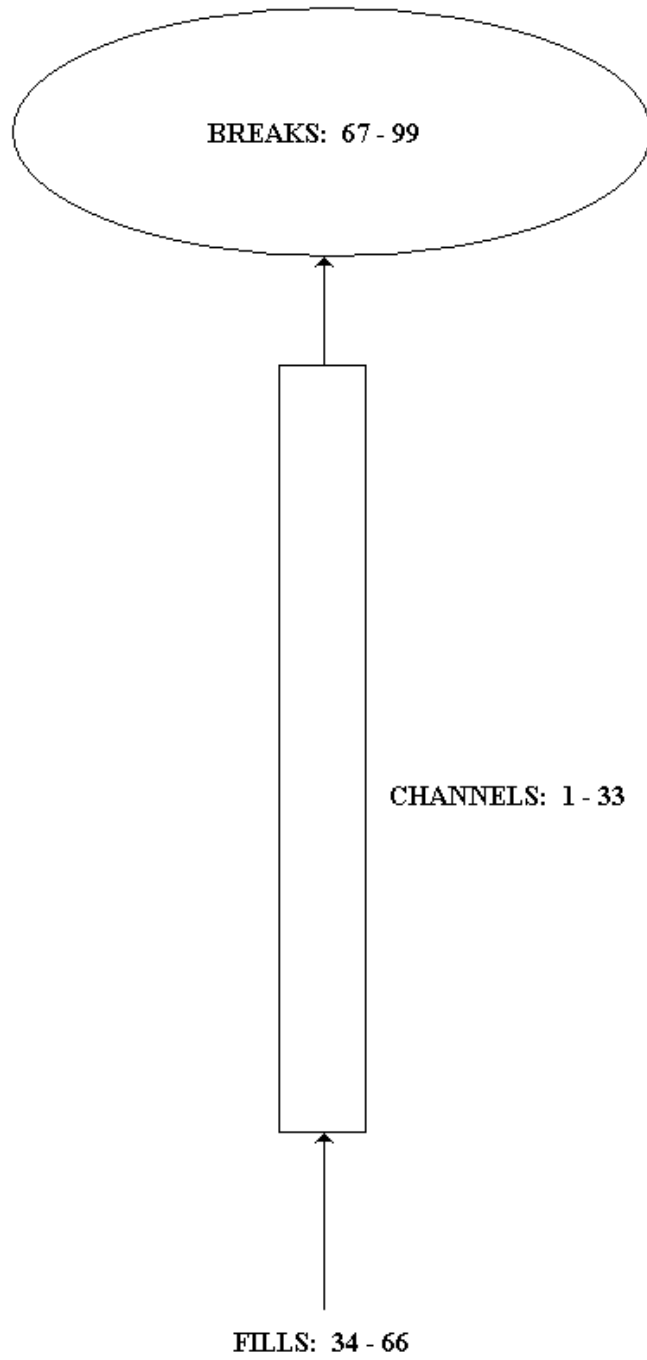
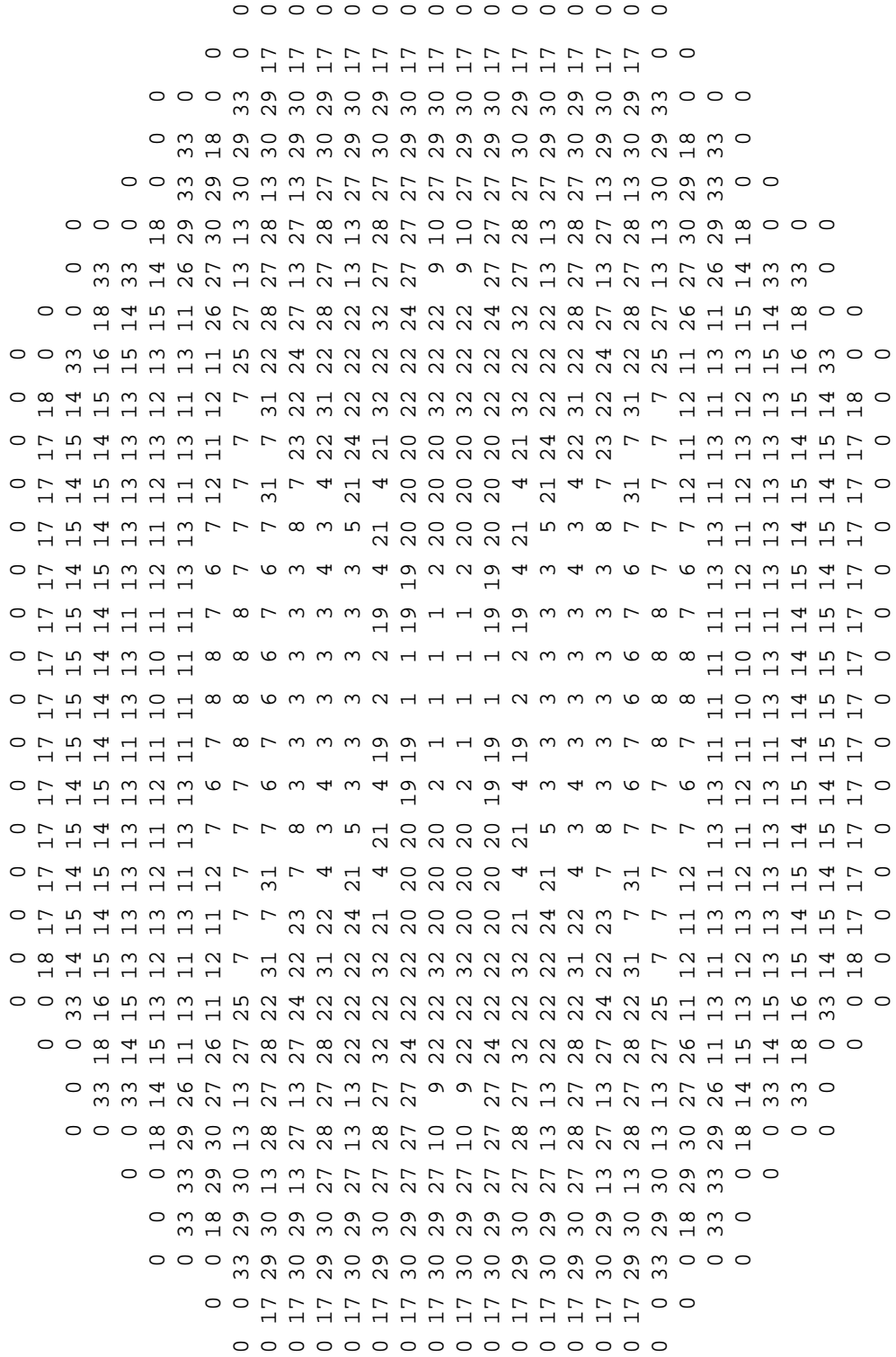


Figure 3.2.2 PB2 Reactor Core Thermal-Hydraulic Channel Radial Map



Chapter 4

NEUTRONIC/THERMAL-HYDRAULIC COUPLING

The feedback, or coupling, between neutronics and thermal-hydraulics can be characterized by choosing user supplied mapping schemes (spatial mesh overlays) in the radial and axial core planes.

Some of the inlet perturbations (inlet disturbances of both temperature and flow rate) are specified as a fraction of the position across the core inlet. This requires either a 3-D modelling of the vessel, or some type of a multi-channel model. The PSU developed core multi-channel model consists of a 33-channel to represent the 764 fuel assemblies of the PB2 reactor core. The above core thermal-hydraulic model was built according to different criteria. First, the fuel assemblies are ranked according to the inlet orifice characteristics. A second criterion is the fuel assembly type (e.g., 7x7 or 8x8). Finally, thermal-hydraulic conditions are also considered (e.g., fuel assembly power, mass flow, etc.).

For the purposes of this benchmark (Exercises 2 and 3), it is recommended that an assembly flow area of 15.535 in² (1.0023E⁻⁰² m²) for fuel assemblies with 7x7 fuel rod arrays, and 15.5277 in² (1.0017E⁻⁰² m²) for fuel assemblies with 8x8 fuel rod arrays are used in the core thermal-hydraulic multi-channel models. There are 764 fuel assemblies in the PB2 reactor core. At EOC 2, there are 576 fuel assemblies of 7x7 type, and 188 of the 8x8 type. The radial distribution of assembly types is shown in Figure 2.4.2 where the assembly types from 1 to 4 identify a fuel assembly with 8x8 fuel arrays and the assembly types from 5 to 18 identify a fuel assembly with 7x7 fuel rod arrays. The core hydraulic characteristics (e.g., core pressure drop) can be found in Ref. [2].

CHAPTER 5

TT Problem

5.1 Description of TT2 scenario

A Turbine Trip (TT) is characterized by a sudden closure of the turbine stop valve (TSV). It can be initiated by a number of turbine or nuclear system malfunctions. An initiating signal could be a high level of condensates in the separators and heaters drain, high vibrations, TSV closure carried out by the reactor operator, condenser low-vacuum, and reactor high liquid level. TSV closure causes a sudden reduction of steam flow, which results in a nuclear system pressure increase. The system pressure increase due to the TT is mitigated by the reactor protection system functions. At high power levels, a TSV closure produces a reactor scram, a turbine bypass valve (BPV) opening and, on some plants, a prompt recirculation pump trip (prompt RPT). At lower initial power levels, the scram initiated by the TSV closure is bypassed if the measured power level indicates the transient can be handled by the turbine bypass system. The safety and relief valves (SRVs) and the BPVs help in releasing the steam production and in limiting the nuclear system pressure increase. On plants which have prompt RPT or if the anticipated transient without scram (ATWS-RPT) set point is reached, the increase of the reactor water level, because of the RPT, can reach the high water level trip set point and trip the feedwater system. Following the feedwater system trip, the reactor water level will drop to the low water level set point, which will initiate the high-pressure emergency systems.

A TT transient in a BWR type reactor is considered one of the most complex events to be analyzed because it involves the reactor core, the high pressure coolant boundary, associated valves and piping in highly complex interactions with variables changing very rapidly.

As it was mentioned, the transient begins with a sudden TSV closure, which initiates a pressure wave in the main steam system, which is quickly transmitted to the reactor pressure vessel. While the TSVs are closing, the bypass system valves are designed to open allowing a steam release and therefore a pressure relief. SRVs can begin to open at prestablished set points, giving additional pressure relief. The pressure wave requires a detailed nodal modeling of the steam system and its associated valves to assure that timing effects and pressure wave magnitude can be accurately determined. This assures to have a pressure history in each valve allowing an adequate modeling of steam flow through each valve.

As the steam pressure increase reaches the reactor pressure vessel, its path must be modeled from the steam dome through the dryers and steam separators, and through the downcomer region to the recirculation system and jet pumps. Accurate representation assures that the induced core pressure oscillations affect the core voids and the core fluid flow in the correct way. Modeling each of the above regions requires special care to assure an adequate simulation of the pressure increase during the transient. Having adequate modeling of the pressure increase assures that the correct core response is calculated.

5.2 Initial steady-state conditions

TT2 initial conditions

The initial steady-state reference data are based on those provided in the EPRI reports [2,3]. For the TT2 transient test, the dynamic measurements were taken with high-speed digital acquisition system capable of sampling over 150 signals every 6 milliseconds. The core power distribution measurements were taken from the plant's local in-core flux detectors. Special fast response pressure and differential pressure transducers were installed in parallel with the existing plant instruments in the nuclear steam supply system. Table 5.2.1 provides the reactor initial conditions for performing steady-state calculations. Figure 5.2.1 shows the PB2 EOC2 TT2 initial control rod pattern. The units of the numbers shown in the control rod map are called notches. One notch equals a length of 3 inches. Table 5.2.2 provides the process computer P1 edit for initial core axial relative power distribution in exercise 1, and for comparison purposes for exercises 2 and 3.

Initial water level above vessel zero (AVZ) is equal to 557 inches (14.1478 m). This measured level is the actual level inside the steam dryer shroud. The initial level AVZ is equal to 564 inches (14.3256 m) for the narrow range measurement outside steam dryer shroud. AVZ is the lowest interior elevation of the vessel (bottom of lower plenum).

HZP initial conditions

The initial conditions for performing PB2 hot zero power (HZP) core calculations are given in Table 5.2.3. The fixed thermal-hydraulic variables should be equally distributed through the whole core. The initial power corresponds to 1% of the PB2 nominal power. Figure 5.2.2 shows the HZP control rod pattern that should be used for the analysis of this calculation. The initial conditions presented in table 5.2.3 along with the control rod pattern shown in Figure 5.2.2 should produce a critical or very-near-to-critical reactor core. A similar control rod grouping approach as shown in Figure 2.4.1 could be used to set up the control rod-mapping scheme for just two control rod groups.

5.3 Transient calculations

Most of the important phenomena of interest during TT2 happened in the first 5 seconds. Therefore, the transient will be simulated for this time period. This approach simplifies the number of components required for performing the analysis of TT2. TSV closure characteristics are presented in Table 5.3.1. Basically, the transient begins with the closure of the TSV. At some point in time, the turbine BPV begins to open. Table 5.3.2 shows the BPV characteristics during the transient. The only boundary conditions imposed in the analysis should be limited to the opening and closure of the above valves. Also, if the opening set points of the SRVs are reached, these valves should be included in the model. Feedwater system behavior during the transient is shown in Table 5.3.3. The normalized relative fission power vs. time data for performing Exercise 1 is available at the benchmark **ftp** site under the directory **Specifications**. The file name is **nfpower_exercise1**.

According to Table 3-6 of reference [3], the actual average planar range monitor (APRM) high flux scram set point should be set to 95% of rated power or 3128.35 MWt. Table 5.3.4 shows the scram initiation time and the delay time that should be used for performing of Exercises 2 and 3. Table 5.3.5 shows the average control rod density (CRD) position during reactor scram. This table can be used for the 1-D neutronic calculation of the transient. An average velocity can be obtained from Table 5.3.5 for the scram modeling in the 3-D kinetics case. An approximate value

obtained from the above table is 2.34 ft/s (0.713 m/s) for the first 0.04 seconds and 4.67 ft/s (1.423 m/s) thereafter. Table 5.3.6 shows the time delays between the initiation of the TSV motion and the pressure responses along the steam line and in the reactor vessel. These values can be used to evaluate the steam line models used in the different code system simulations. Some available TT2 transient test peak measured values are presented in Table 5.3.7. Some TT2 test data acquisition instrument time delays are given in Table 5.3.8.

The neutronics and thermal-hydraulic information presented in Chapters 1 through 5, suffices for performing Exercises 1, 2, and 3. In addition, extreme versions of Exercise 3 are defined as follows:

1. Turbine trip without bypass system relief opening (would increase the power peak and provide enough pressurization for safety/relief valve opening).

To perform this Exercise, the participants should inactivate the BPV opening in their thermal-hydraulic modeling. Everything else should remain the same as for Exercise 3

2. Turbine trip without scram (would increase the power peak and produce a second power peak and would be a challenge to the coupled code predictions).

No credit for scram is taken during this exercise. To perform this calculation, the participants should inactivate the reactor scram by simply specifying a large number for scram initiation. Everything else should remain the same as for Exercise 3.

3. Combined extreme scenario – turbine trip with bypass system relief failure and without reactor scram. Some preliminary results indicated that this case is very close to a super-prompt-critical state and make a good case for code-to-code comparisons).

To perform this Exercise, both reactor scram and BPV opening should be inactivated. Everything else should remain the same as for Exercise 3.

Table 5.2.1 PB2 TT2 initial conditions from process computer P1 edit

Core thermal power, MWt	2030
Initial power level, % of rated	61.65
Gross power output, MWe	625.1
Feedwater flow, kg/s	980.26
Reactor pressure, Pa	6798470.0
Total core flow, kg/s	10445.0
Core inlet subcooling, J/kg	48005.291
Core pressure drop (calculated), Pa	113560.7
Core pressure drop (measured), Pa	83567.4
Jet pump driving flow, kg/s	2871.24*
Core average exit quality, fraction	0.097
Core average void fraction, fraction	0.304
Core average power density, kW/l	31.28
Control density, fraction	0.159

* - Corrected for calibration and conversion errors

Table 5.2.2 PB2 TT2 initial core axial relative power from process computer P1 edit

Node Number	Axial Location, (cm)	Relative power
1	7.62	0.308051
2	22.86	0.616103
3	38.1	0.707754
4	53.34	0.773947
5	68.58	0.814681
6	83.82	0.880874
7	99.06	0.972526
8	114.3	1.066723
9	129.54	1.163467
		1.26021

10	144.78	1.356953
11	160.02	1.407871
12	175.26	1.412963
13	190.5	1.402779
14	205.74	1.37732
15	220.98	1.328949
16	236.22	1.257664
17	251.46	1.188925
18	266.7	1.122733
19	281.94	1.031081
20	297.18	0.913971
21	312.42	0.763764
22	327.66	0.58046
23	342.9	0.29023
24	358.14	

Table 5.2.3 PB2 HZP initial conditions	
Fuel Temperature, K	552.833
Average Coolant density, kg/m ³	753.9777
Reactor Power, MW	32.93

Table 5.3.1 TSV Flow Fraction vs. Time	
Time (sec)	Flow (fraction)
0.000	1.0000
0.010	0.9995
0.020	0.9985
0.030	0.9970
0.040	0.9950
0.050	0.9930
0.054	0.9900
0.061	0.9500
0.066	0.8600
0.068	0.7600
0.078	0.3200
0.086	0.1450
0.096	0.0000
1.00	0.000
5.00	0.000

Table 5.3.2 Bypass Valve Position vs. Time	
Time (sec)	Position (%)
0.000	0.0000
0.054	0.0000
0.072	0.4100
0.090	0.7100
0.102	2.3500
0.138	8.9700
0.162	8.9700
0.222	15.720
0.300	29.490
0.504	62.760
0.672	88.170
0.732	91.430
0.846	100.00
5.000	100.00

Table 5.3.3 Feedwater Flow vs. Time	
Time (sec)	Flow (lbm/sec)
0.0	2171.0
0.4	2171.0
0.5	2165.0
1.0	2005.0
1.5	2000.0
2.0	1920.0
2.5	1900.0
3.0	1950.0
3.5	2030.0
4.0	2220.0
4.5	2485.0
5.0	2760.0

Table 5.3.4 PB2 TT2 Scram Characteristics	
APRM high flux scram set-point, % Rated	95 (3128.35 MWt)
Time delay prior to rod motion, msec	120
Time of scram initiation, sec	0.63
Initiates CR insertion, sec	0.75

Table 5.3.5 CRD Position After Scram vs. Time	
Time (sec)	Position (ft)
0.000	0.0000
0.120	0.0000
0.160	0.0935
0.247	0.5000
0.354	1.0000
0.457	1.5000
2.500	10.200
3.080	12.000
5.000	12.000

Table 5.3.6 PB2 TT2 Event Timing (time delay in msec)	
TSV begin to close	0
TSV closed	96
Begin bypass opening	72
Bypass full open	846
Turbine pressure initial response	
A. Steam line	102
B. Steam line	126
Steam line pressure initial response	
A. Steam line	348
D. Steam line	378
Vessel pressure initial response	432
Core exit pressure initial response	486

Table 5.3.7 PB2 TT2 Peak Measure Responses	
Average neutron flux (% Rated)	279
Core exit pressure (psia)	1034
Reactor vessel pressure (psia)	1038

Table 5.3.8 TT2 test acquisition instrument time delays (in msec)	
Core upper plenum	60
Steam Dome	50
Turbine inlet	45

**Figure 5.2.1. PB2 TT2 Initial control rod pattern
(48 – full withdrawn, 0 – full insertion)**

59				48	48	48	48	48	48	48					
55			48	48	34	48	36	48	34	48	48				
51			48	48	0	48	26	48	26	48	0	48	48		
47		48	48	40	48	36	48	32	48	36	48	40	48	48	
43	48	48	0	48	26	48	4	48	4	48	26	48	0	48	48
39	48	34	48	36	48	48	48	48	48	48	48	36	48	34	48
35	48	48	26	48	4	48	32	48	32	48	4	48	26	48	48
31	48	36	48	32	48	48	48	48	48	48	48	32	48	36	48
27	48	48	26	48	4	48	32	48	32	48	4	48	26	48	48
23	48	34	48	36	48	48	48	48	48	48	48	36	48	34	48
19	48	48	0	48	26	48	4	48	4	48	26	48	0	48	48
15		48	48	40	48	36	48	32	48	36	48	40	48	48	
11			48	48	0	48	26	48	26	48	0	48	48		
07				48	48	34	48	36	48	34	48	48			
03					48	48	48	48	48	48	48				
	02	06	10	14	18	22	26	30	34	38	42	46	50	54	58

**Figure 5.2.2. PB2 HZP control rod pattern
(48 – full withdrawn, 0 – full insertion)**

59				0	48	0	48	0	48	0					
55				0	48	0	48	0	48	0	48	0			
51				0	48	0	48	0	48	0	48	0	48	0	
47				0	48	0	48	0	48	0	48	0	48	0	
43	0	48	0	48	0	48	0	48	0	48	0	48	0	48	0
39	48	0	48	0	48	0	48	0	48	0	48	0	48	0	48
35	0	48	0	48	0	48	0	48	0	48	0	48	0	48	0
31	48	0	48	0	48	0	48	0	48	0	48	0	48	0	48
27	0	48	0	48	0	48	0	48	0	48	0	48	0	48	0
23	48	0	48	0	48	0	48	0	48	0	48	0	48	0	48
19	0	48	0	48	0	48	0	48	0	48	0	48	0	48	0
15		0	48	0	48	0	48	0	48	0	48	0	48	0	
11			0	48	0	48	0	48	0	48	0	48	0		
07				0	48	0	48	0	48	0	48	0			
03					0	48	0	48	0	48	0				
	02	06	10	14	18	22	26	30	34	38	42	46	50	54	58

Chapter 6

OUTPUT REQUESTED

- Results should be presented on paper and electronic format (diskette, CD, etc).
- All data should be in SI units (kg, m, s).
- For time histories, data should be at 0.006 seconds intervals (for code-to-data comparison)
- For time histories, data should be at 0.05 seconds intervals (for code-to-code comparison)

6.1 Initial steady-state results

The following steady state results will be compared for **Exercises 1 and 3**:

- Core average axial void fraction distribution
- Core axial pressure drop
- Core inlet enthalpy

The following results will be compared for the initial test conditions (**Exercises 2 and 3**) and for the HZP state (**Exercise 2**):

- Core averaged relative axial power distribution
- Core averaged axial void fraction distribution (excluding the HZP state)
- Radial power distribution – two-dimensional assembly normalized power distribution (for the 3-D kinetics options)
- K_{eff}
- Relative power distributions for fuel assemblies 75 (rodded bundle) and 367 (unrodded bundle) - numbering the core fuel region from top-to-bottom and from left to right (see fuel region on Figure 2.2.1).

6.2 Transient results

Exercise 1, 2, and 3

- Sequence of events:
 - Turbine stop valve closed, s
 - Bypass valve begins opening, s
 - Bypass full open, ms
 - Vessel (dome) pressure initial response, s
 - Core exit pressure initial response, s
 - Safety/relief valve opening, s
 - Safety/relief valve closing, s
- Time histories:
 - Total reactor core fission power
 - Dome pressure

- Core exit pressure
- Total jet pump flow

Exercises 2 and 3 (3-D kinetics version)

For the Exercises 2 and Exercise 3 (3-D kinetics option), a comparison against LPRM measurements is performed. The participants are provided with an LPRM response model, which is described in Chapter 2. The necessary neutronic data is included in the 3-D cross-section library as it is described in Chapter 2. For comparison purposes, just the averaged time history values are requested from the participants at the four different levels: A, B, C, and D.

- Transient peaked measured response:
 - Averaged neutron flux, (% rated)
 - Core exit pressure, MPa
 - Reactor vessel (dome) pressure, Mpa
 - Maximum power after reactor scram
- Transient snapshots (radial and axial normalized core power distributions) plus relative power distributions at the specified bundle locations (75 and 367):
 - At time of maximum power before reactor scram
 - At time of maximum power after reactor scram
 - At the end of the transient (5 seconds for normal Exercises, 10 seconds for extreme versions of Exercise 3)

6.3 Output format

Results may be sent via e-mail to kni1@psu.edu or on diskette to Kostadin N. Ivanov, Nuclear Engineering Program, 230 Reber Building, University Park, PA. 16802, U.S.A.

Diskette should be in PC 3.5" (720 KB or 1.44 MB) format, containing one text (ASCII) file for each exercise, named RESULTS.A, RESULTS.B, and RESULTS.C respectively. Contents should be typed as close as possible to sample format.

Remarks:

- Time histories consist of data records (time, value, value), one per line, starting at 0 seconds, up to 5 seconds (10 seconds for the extreme versions of Exercise 3). Please provide the units on the first line.
- Radial and axial profiles should be given according to the form shown in Figures 6.1 and 6.2.
- Please do not use tabs in the data files.
- Start each line in column one and end each line with a carriage return <CR>.

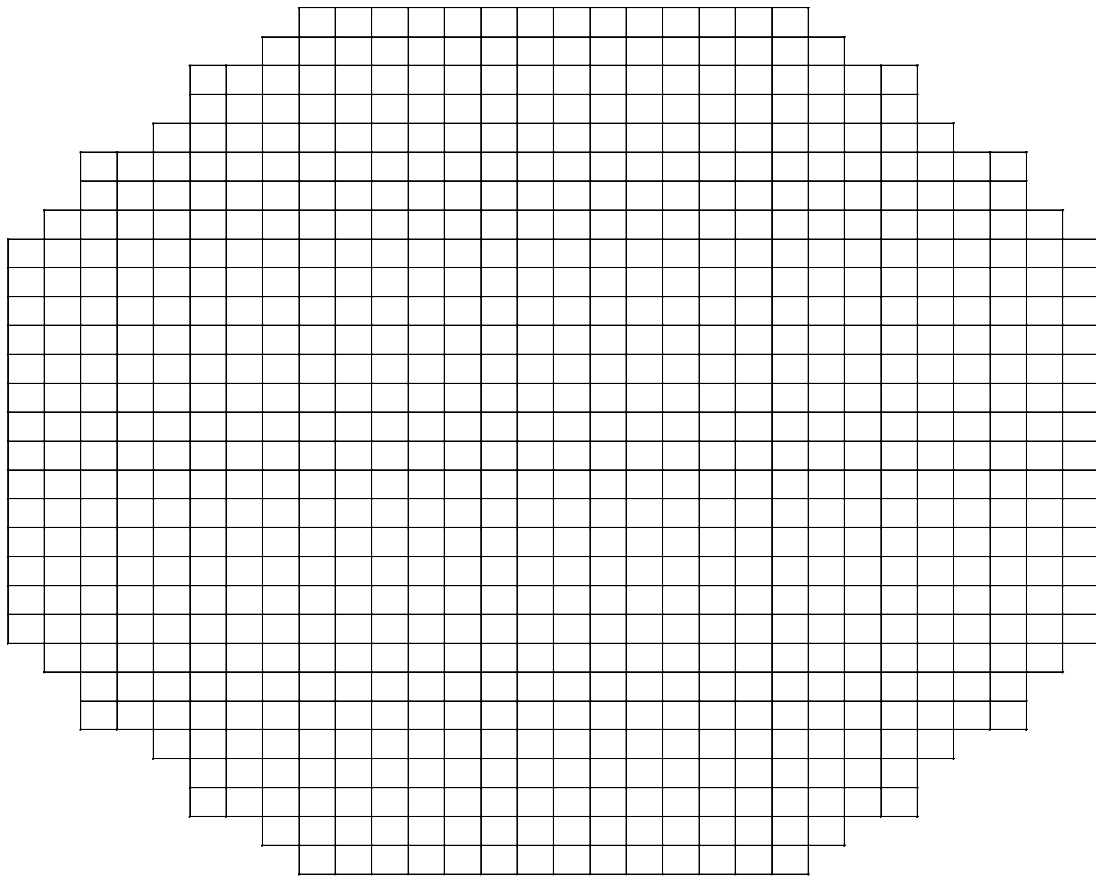


Figure 6.1 Form for axial power distribution

Bottom

1	2	3	4	5	6	7	8	9	10	11	12

13	14	15	16	17	18	19	20	21	22	23	24

Top

Figure 6.2 Form for radial power distribution

Output sample:

1 PEACH BOTTOM TURBINE TRIP BENCHMARK RESULTS FROM CODE
"XXXXXXXX", EXERCISE 3

2 STEADY STATE RESULTS

2.1 $K_{\text{eff}}=1.00000$

2.2 Radial power distribution (full core) – start each line in column one, leave a blank space
in between each number, and use a total of six spaces per number:

```
          0.9999 0.9999 0.9999 0.9999 0.9999
        0.9999 0.9999 0.9999 0.9999 0.9999 0.9999 0.9999 0.9999
      0.9999 0.9999 0.9999 0.9999 0.9999 0.9999 0.9999 0.9999 0.9999
    0.9999 0.9999 0.9999 0.9999 0.9999 0.9999 0.9999 0.9999 0.9999 0.9999
  0.9999 0.9999 0.9999 0.9999 0.9999 0.9999 0.9999 0.9999 0.9999 0.9999
0.9999 0.9999 0.9999 0.9999 0.9999 0.9999 0.9999 0.9999 0.9999 0.9999 0.9999
0.9999 0.9999 0.9999 0.9999 0.9999 0.9999 0.9999 0.9999 0.9999 0.9999 0.9999
0.9999 0.9999 0.9999 0.9999 0.9999 0.9999 0.9999 0.9999 0.9999 0.9999 0.9999
0.9999 0.9999 0.9999 0.9999 0.9999 0.9999 0.9999 0.9999 0.9999 0.9999 0.9999
0.9999 0.9999 0.9999 0.9999 0.9999 0.9999 0.9999 0.9999 0.9999 0.9999 0.9999
0.9999 0.9999 0.9999 0.9999 0.9999 0.9999 0.9999 0.9999 0.9999 0.9999 0.9999
0.9999 0.9999 0.9999 0.9999 0.9999 0.9999 0.9999 0.9999 0.9999 0.9999 0.9999
0.9999 0.9999 0.9999 0.9999 0.9999 0.9999 0.9999 0.9999 0.9999 0.9999 0.9999
0.9999 0.9999 0.9999 0.9999 0.9999 0.9999 0.9999 0.9999 0.9999 0.9999 0.9999
0.9999 0.9999 0.9999 0.9999 0.9999 0.9999 0.9999 0.9999 0.9999 0.9999 0.9999
0.9999 0.9999 0.9999 0.9999 0.9999 0.9999 0.9999 0.9999 0.9999 0.9999 0.9999
```

2.3 Axial power distribution – place all data starting in column one, leave a blank in between
each number, and use a total of six spaces per number:

```
0.9999 0.9999 0.9999 0.9999 0.9999 0.9999 0.9999 0.9999 0.9999 0.9999 0.9999
0.9999 0.9999 0.9999 0.9999 0.9999 0.9999 0.9999 0.9999 0.9999 0.9999 0.9999
```

2.4 Core averaged axial void fraction distribution – use the same format as for the axial
power distribution.

3 SEQUENCE OF EVENTS

Table 6.3.1 Sequence of events output

Event description	Time (seconds)
Turbine stop valve closed	
Bypass valve begins opening	
Bypass full open	
Vessel (dome) pressure initial response	
Core exit pressure initial response	
Safety/relief valve opening (Extreme Cases of Exercise 3)	
Safety/relief valve closing (Extreme Cases of Exercise 3)	
High flux set point reached	

4 TRANSIENT TIME HISTORIES

The first column of numbers should be the time covering a time interval from 0 to 5 seconds, with data taken every 0.006 seconds. The second, third, fourth, and fifth column should be core power, dome pressure, core exit pressure, and total jet pump flow respectively; at that time, with a space between the columns. Time histories for the extreme cases of Exercise 3 should cover a time interval from 0 to 10 seconds, with data taken every 0.05 seconds. Same column format as above should be used for the time history variables.

REFERENCES

1. K. Ivanov, et al “PWR Main Steam Line Break (MSLB) Benchmark. Volume 1: Final Specifications”, NEA/NSC/DOC(99)8. April 1999.
2. N. H. Larsen, “Core Design and Operating Data for Cycles 1 and 2 of Peach Bottom 2”, EPRI NP-563, June 1978.
3. L. A. Carmichael and R. O. Niemi, “Transient and Stability Tests at Peach Bottom Atomic Power Station Unit 2 at End of Cycle 2”, EPRI NP-564, June 1978.
4. A. M. Olson, Topical Report PECo-FMS-0004-A, “Methods for Performing BWR System Transient Analysis”, Philadelphia Electric Company, (1988).

APENDIX A

SKELETON INPUT DECK

SKELETON INPUT DECK

NVOL
53

NJUN
66

VOLUMES:

# VOLUME	DESCRIPTION
1	LOWER PLENUM - LPM
2	CORE INLET VOLUME - CIV
3	CORE BYPASS
4	UPPER CORE PLENUM - UPM
5	STANDPIPES
6	STEAM SEPARATORS - SS
7	STEAM DOME
8	UPPER DOWNCOMER - UDC
9	MIDDLE DOWNCOMER - MDC
10	LOWER DOWNCOME - LDC
11	RECIRC SUCTION 'A'
12	RECIRC SUCTION 'B'
13	RECIRC PUMP 'A'
14	RECIRC PUMP 'B'
15	RECIRC DISCHARGE 'A'
16	RECIRC DISCHARGE 'B'
17	JET PUMP 'A'
18	JET PUMP 'B'
50	MAIN STEAM LINE 1
51	MAIN STEAM LINE 2
52	MAIN STEAM LINE 3
53	MAIN STEAM LINE 4

54	MAIN STEAM LINE 5
55	MAIN STEAM LINE 6
101	CORE 1
102	CORE 2
103	CORE 3
104	CORE 4
105	CORE 5
106	CORE 6
107	CORE 7
108	CORE 8
109	CORE 9
110	CORE 10
111	CORE 11
112	CORE 12
113	CORE 13
114	CORE 14
115	CORE 15
116	CORE 16
117	CORE 17
118	CORE 18
119	CORE 19
120	CORE 20
121	CORE 21
122	CORE 22
123	CORE 23
124	CORE 24
125	CORE EXIT VOLUME
200	STEAM BYPASS CHEST

201	STEAM BYPASS LINES
202	STEAM BYPASS ORIFICE
500	CONDENSER

Reactor Vessel					
#	Volume	ZVolume	FlowA	DiamV	Elev
1	2064.951	17.28125	119.49084	0.791085	0
2	106.0898	1.196067	88.698869	0.372351	5.17023287
3	965.9736	14.475	69.055861	0.170615	5.267389051
4	953.0751	5	190.61502	15.5788	9.667992563
5	377.5064	8.9177	42.332261	0.505417	10.83291667
6	681.5879	6.166667	91.669802	0.74375	13.55106468
7	6292.622	22.31771	281.95647	18.94725	15.43068764
8	1919.922	9.083333	204.79822	1.091352	12.66205407
9	1721.338	9.963541	238.70411	2.11053	10.51414045
10	2241.127	24.34896	92.042004	2.791474	3.092487503
17	125.6451	16.43333	7.6457436	1.00E+20	3.0353369
18	125.6451	16.43333	7.6457436	1.00E+20	3.0353369
101	41.97954	0.5	83.959069	0.044608	5.494404414
102	41.97954	0.5	83.959069	0.044608	5.646806267
103	41.97954	0.5	83.959069	0.044608	5.79920812
104	41.97954	0.5	83.959069	0.044608	5.951609973
105	41.97954	0.5	83.959069	0.044608	6.104011826
106	41.97954	0.5	83.959069	0.044608	6.25641368
107	41.97954	0.5	83.959069	0.044608	6.408815533
108	41.97954	0.5	83.959069	0.044608	6.561217386
109	41.97954	0.5	83.959069	0.044608	6.713619239
110	41.97954	0.5	83.959069	0.044608	6.866021092
111	41.97954	0.5	83.959069	0.044608	7.018422946
112	41.97954	0.5	83.959069	0.044608	7.170824799
113	41.97954	0.5	83.959069	0.044608	7.323226652
114	41.97954	0.5	83.959069	0.044608	7.475628505
115	41.97954	0.5	83.959069	0.044608	7.628030358
116	41.97954	0.5	83.959069	0.044608	7.780432212
117	41.97954	0.5	83.959069	0.044608	7.932834065
118	41.97954	0.5	83.959069	0.044608	8.085235918
119	41.97954	0.5	83.959069	0.044608	8.237637771
120	41.97954	0.5	83.959069	0.044608	8.390039624
121	41.97954	0.5	83.959069	0.044608	8.542441478
122	41.97954	0.5	83.959069	0.044608	8.694843331
123	41.97954	0.5	83.959069	0.044608	8.847245184
124	41.97954	0.5	83.959069	0.044608	8.999647037
125	142.1182	1.692708	83.959069	0.044608	9.152048891

Recirculation Loops					
#	Volume	ZVolume	FlowA	DiamV	Elev
11	233.9687	42.05208	3.6502301	2.155833	-8.239225189
12	233.9687	42.05208	3.6502301	2.155833	-8.239225189
13	49.67949	3.077917	3.6502301	2.155833	-7.188287308
14	49.67949	3.077917	3.6502301	2.155833	-7.188287308
15	306.8175	51.08117	2.8411115	0.524994	-6.892373811
16	306.8175	51.08117	2.8411115	0.524994	-6.892373811

Steam Lines and Steam Bypass System					
#	Volume	ZVolume	FlowA	DiamV	Elev
050	634.0143	46.51042	12.199428	1.970583	2.549555992
051	594.8101	18.41667	12.199428	1.970583	-3.063912156
052	1064.168	17.54871	12.199428	1.970583	-3.346769995
053	964.0202	2.220583	12.199428	1.970583	1.299921665
054	901.7411	2.220583	12.199428	1.970583	1.223721044
055	1163.289	2.720583	12.199428	1.970583	0.995095221
200	216.2789	5.25	2.9781592	1.323024	1.295415752
201	484.4076	37.91146	2.8539713	0.635417	-9.821981834
202	16.71875	0.88182	5.4965753	0.88182	-9.956372836
500	1.00E+20	50	1.00E+09	1.00E+09	-15.24018532

JUNCTIONS:

Junction #	DESCRIPTION
001	JET PUMP 'A' DISCHARGE
002	JET PUMP 'B' DISCHARGE
003	LPM TO CORE INLET VOL.
004	LOWER PLENUM TO BYPASS
005	CORE INLET TO BYPASS
006	BYPASS TO UPPER PLENUM
007	UPPER PLENUM TO STANDPIPES
008	STANDPIPES TO SS
009	SS TO STEAM DOME
010	SS TO MDC
011	UDC TO STEAM DOME
012	UDC TO MDC
013	MDC TO LDC
014	JET PUMP 'B' SUCTION'
015	JET PUMP 'A' SUCTION'
016	RECIRC 'B' SUCTION
017	RECIRC 'A' SUCTION
018	PUMP 'B' SUCTION
019	PUMP 'A' SUCTION
020	PUMP 'B' DISCHARGE
021	PUMP 'A' DISCHARGE

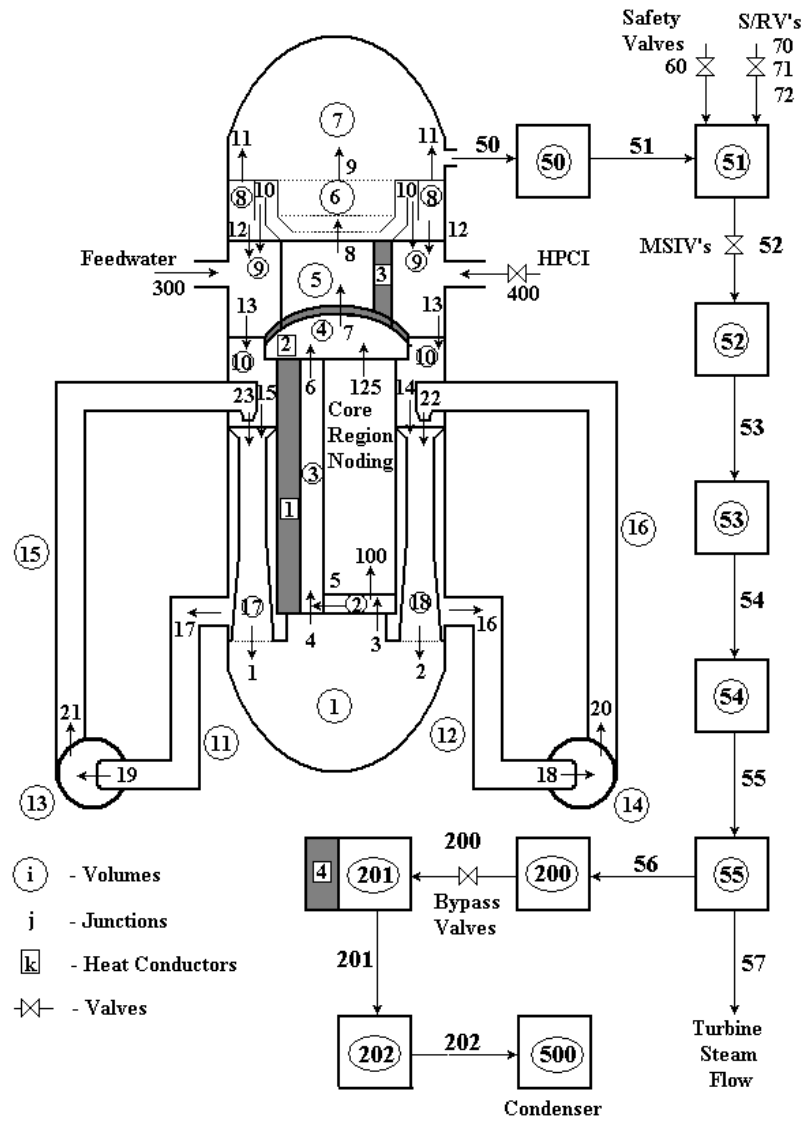
022	JET PUMP 'B' DRIVE
023	JET PUMP 'A' DRIVE
050	STEAM DOME TO MN STM L1
051	MN STM L1 TO MN STM L2
052	MN STM L2 TO MN STM L3
053	MN STM L3 TO MN STM L4
054	MN STM L4 TO MN STM L5
055	MN STM L5 TO MN STM L6
056	MS STM L6 TO STM BYPASS
057	MAIN STOP VALVES
060	SAFETY VALVES
070	SAFETY RELIEF VALVE GRP 1
071	SAFETY RELIEF VALVE GRP 2
072	SAFETY RELIEF VALVE GRP 3
100	CORE INLET TO CORE 1
101	CORE 1 TO CORE 2
102	CORE 2 TO CORE 3
103	CORE 3 TO CORE 4
104	CORE 4 TO CORE 5
105	CORE 5 TO CORE 6
106	CORE 6 TO CORE 7
107	CORE 7 TO CORE 8
108	CORE 8 TO CORE 9
109	CORE 9 TO CORE 10
110	CORE 10 TO CORE 11
111	CORE 11 TO CORE 12
112	CORE 12 TO CORE 13
113	CORE 13 TO CORE 14
114	CORE 14 TO CORE 15
115	CORE 15 TO CORE 16
116	CORE 16 TO CORE 17
117	CORE 17 TO CORE 18
118	CORE 18 TO CORE 19
119	CORE 19 TO CORE 20
120	CORE 20 TO CORE 21
121	CORE 21 TO CORE 22
122	CORE 22 TO CORE 23
123	CORE 23 TO CORE 24
124	CORE 24 TO CORE EXIT
125	CORE EXT TO UPM
200	STEAM BYPASS VALVES
201	STEAM BYPASS ORIFICE
202	STEAM BYPASS TO CONDENSER
300	FEEDWATER NFILL
400	HPCI

Reactor Vessel				
#	Frm	To	JnArea	JnElev
1	17	1	21.81662	9.958333
2	18	1	21.81662	9.958333
3	1	2	19.00019	16.9625
4	1	3	0.29	17.28125
5	2	3	1.71	18
6	3	4	44.12424	31.71875
7	4	5	42.33226	35.54063
8	5	6	42.33226	44.45833
9	6	7	60.49032	50.625
10	6	9	136.5707	44.45833
11	8	7	283.1268	50.625
12	8	9	156.5359	41.54167
13	9	10	79.6361	34.49479
14	10	18	2.7	26.39167
15	10	17	2.7	26.39167
18	12	14	3.65023	-23.5833
19	11	13	3.65023	-23.5833
20	14	16	3.65023	-20.5054
21	13	15	3.65023	-20.5054
100	2	101	83.95907	18.02604
101	101	102	83.95907	18.52604
102	102	103	83.95907	19.02604
103	103	104	83.95907	19.52604
104	104	105	83.95907	20.02604
105	105	106	83.95907	20.52604
106	106	107	83.95907	21.02604
107	107	108	83.95907	21.52604
108	108	109	83.95907	22.02604
109	109	110	83.95907	22.52604
110	110	111	83.95907	23.02604
111	111	112	83.95907	23.52604
112	112	113	83.95907	24.02604
113	113	114	83.95907	24.52604
114	114	115	83.95907	25.02604
115	115	116	83.95907	25.52604
116	116	117	83.95907	26.02604
117	117	118	83.95907	26.52604
118	118	119	83.95907	27.02604
119	119	120	83.95907	27.52604
120	120	121	83.95907	28.02604
121	121	122	83.95907	28.52604
122	122	123	83.95907	29.02604
123	123	124	83.95907	29.52604
124	124	125	83.95907	30.02604
125	125	4	83.95907	31.71875

Recirculation Loops				
#	Frm	To	JnArea	JnElev
16	10	12	7.669904	13.45833
17	10	11	7.669904	13.45833
18	12	14	3.65023	-23.5833
19	11	13	3.65023	-23.5833
20	14	16	3.65023	-20.5054
21	13	15	3.65023	-20.5054
22	16	18	0.46	26.39167
23	15	17	0.46	26.39167

Steam Lines				
#	Frm	To	JnArea	JnElev
50	7	50	12.19943	54.875
51	50	51	12.19943	8.364583
52	51	52	12.19943	-10.0521
53	52	53	12.19943	4.264708
54	53	54	12.19943	4.264708
55	54	55	12.19943	5
56	55	200	3.408846	4.25
57	0	55	1	4.25
60	0	51	0.27053	8
70	0	51	0.532404	8
71	0	51	0.532404	8
72	0	51	0.399303	8
200	200	201	1	5.6875
201	201	202	0.659611	-31.9375
202	202	500	1.884505	-31.9375
300	0	9	1	41.54167
400	0	9	1	41.54167

Figure A.1. RETRAN nodalization diagram



APPENDIX B

Sample cross-section table

```

*
* NEM-Cross Section Table Input
*
*   T Fuel      Rho Mod.
*     6         6
*
*****
*           X-Section set #      1
*
*   Group No.  1
*
***** Diffusion Coefficient Table
*
.4000000E+03 .8000000E+03 .1200000E+04 .1600000E+04 .1800000E+04
.2400000E+04 .1415950E+03 .2261546E+03 .2996453E+03 .4350457E+03
.5991722E+03 .7794058E+03 .2007900E+01 .2014100E+01 .2020100E+01
.2026000E+01 .2029000E+01 .2037700E+01 .1897700E+01 .1903800E+01
.1909700E+01 .1915600E+01 .1918500E+01 .1927200E+01 .1810700E+01
.1816700E+01 .1822600E+01 .1828400E+01 .1831300E+01 .1839900E+01
.1668800E+01 .1674600E+01 .1680300E+01 .1686000E+01 .1688800E+01
.1697200E+01 .1522700E+01 .1528300E+01 .1533800E+01 .1539200E+01
.1542000E+01 .1550100E+01 .1383400E+01 .1388600E+01 .1393800E+01
.1399000E+01 .1401600E+01 .1409300E+01
*
***** Absorption X-Section Table
*
.4000000E+03 .8000000E+03 .1200000E+04 .1600000E+04 .1800000E+04
.2400000E+04 .1415950E+03 .2261546E+03 .2996453E+03 .4350457E+03
.5991722E+03 .7794058E+03 .5733400E-02 .5842800E-02 .5927800E-02
.5997400E-02 .6028100E-02 .6107000E-02 .6023500E-02 .6145400E-02
.6240400E-02 .6318300E-02 .6352700E-02 .6441400E-02 .6235400E-02
.6366900E-02 .6469400E-02 .6553700E-02 .6590900E-02 .6687000E-02
.6535600E-02 .6679800E-02 .6792600E-02 .6885600E-02 .6926700E-02
.7033400E-02 .6807400E-02 .6961600E-02 .7082700E-02 .7182600E-02
.7227000E-02 .7342100E-02 .7043900E-02 .7206500E-02 .7334500E-02
.7440400E-02 .7487500E-02 .7609700E-02
*
***** Fission X-Section Table
*
.4000000E+03 .8000000E+03 .1200000E+04 .1600000E+04 .1800000E+04
.2400000E+04 .1415950E+03 .2261546E+03 .2996453E+03 .4350457E+03
.5991722E+03 .7794058E+03 .1694519E-02 .1687392E-02 .1680321E-02
.1673479E-02 .1670099E-02 .1660123E-02 .1760207E-02 .1752468E-02
.1744963E-02 .1737541E-02 .1733871E-02 .1723065E-02 .1806831E-02
.1798795E-02 .1790994E-02 .1783276E-02 .1779438E-02 .1768199E-02
.1875604E-02 .1867335E-02 .1859149E-02 .1851046E-02 .1847036E-02
.1835163E-02 .1938822E-02 .1930488E-02 .1922119E-02 .1913830E-02
.1909647E-02 .1897342E-02 .1995480E-02 .1986965E-02 .1978453E-02
.1969863E-02 .1965628E-02 .1952890E-02
*
***** Nu-Fission X-Section Table
*
.4000000E+03 .8000000E+03 .1200000E+04 .1600000E+04 .1800000E+04
.2400000E+04 .1415950E+03 .2261546E+03 .2996453E+03 .4350457E+03
.5991722E+03 .7794058E+03 .4226300E-02 .4209200E-02 .4192400E-02
.4176000E-02 .4167900E-02 .4144000E-02 .4384500E-02 .4366100E-02
.4348100E-02 .4330300E-02 .4321500E-02 .4295600E-02 .4496300E-02
.4477200E-02 .4458500E-02 .4440000E-02 .4430800E-02 .4403700E-02
.4660500E-02 .4640700E-02 .4621100E-02 .4601700E-02 .4592100E-02
.4563500E-02 .4810800E-02 .4790700E-02 .4770700E-02 .4750700E-02
.4740700E-02 .4711100E-02 .4944200E-02 .4923700E-02 .4903200E-02
.4882700E-02 .4872400E-02 .4841800E-02
*
***** Scattering X-Section Table
*
**** From group 1 to 2
.4000000E+03 .8000000E+03 .1200000E+04 .1600000E+04 .1800000E+04
.2400000E+04 .1415950E+03 .2261546E+03 .2996453E+03 .4350457E+03
.5991722E+03 .7794058E+03 .7693100E-02 .7633900E-02 .7583700E-02
.7539000E-02 .7518200E-02 .7460300E-02 .9287200E-02 .9212100E-02
.9147500E-02 .9089500E-02 .9062200E-02 .8986000E-02 .1069300E-01
.1060500E-01 .1052800E-01 .1045900E-01 .1042600E-01 .1033500E-01

```

```

.1333700E-01 .1322600E-01 .1312900E-01 .1304100E-01 .1299900E-01
.1288000E-01 .1661200E-01 .1647700E-01 .1635800E-01 .1624800E-01
.1619500E-01 .1604500E-01 .2043400E-01 .2027500E-01 .2013200E-01
.1999900E-01 .1993500E-01 .1975300E-01
*
***** Assembly Disc. Factor Table - W
*
.4000000E+03 .8000000E+03 .1200000E+04 .1600000E+04 .1800000E+04
.2400000E+04 .1415950E+03 .2261546E+03 .2996453E+03 .4350457E+03
.5991722E+03 .7794058E+03 .9337490E+00 .9346120E+00 .9353030E+00
.9358790E+00 .9361360E+00 .9368150E+00 .9289820E+00 .9298700E+00
.9305890E+00 .9311670E+00 .9314380E+00 .9321550E+00 .9247810E+00
.9257670E+00 .9264880E+00 .9270990E+00 .9273760E+00 .9280960E+00
.9173030E+00 .9181880E+00 .9188970E+00 .9195280E+00 .9198200E+00
.9205860E+00 .9077700E+00 .9086590E+00 .9093830E+00 .9100110E+00
.9103000E+00 .9110590E+00 .8938700E+00 .8947480E+00 .8954810E+00
.8961440E+00 .8964430E+00 .8972790E+00
*
***** Assembly Disc. Factor Table - S
*
.4000000E+03 .8000000E+03 .1200000E+04 .1600000E+04 .1800000E+04
.2400000E+04 .1415950E+03 .2261546E+03 .2996453E+03 .4350457E+03
.5991722E+03 .7794058E+03 .9848210E+00 .9851320E+00 .9853740E+00
.9855810E+00 .9856740E+00 .9859130E+00 .9825030E+00 .9828240E+00
.9830770E+00 .9833260E+00 .9834270E+00 .9836950E+00 .9810430E+00
.9812700E+00 .9815420E+00 .9817760E+00 .9818830E+00 .9821880E+00
.9785220E+00 .9788640E+00 .9791600E+00 .9793880E+00 .9794880E+00
.9797790E+00 .9762050E+00 .9765230E+00 .9767930E+00 .9770250E+00
.9771300E+00 .9774450E+00 .9735190E+00 .9738470E+00 .9741160E+00
.9743250E+00 .9744300E+00 .9746920E+00
*
* Group No. 2
*
***** Diffusion Coefficient Table
*
.4000000E+03 .8000000E+03 .1200000E+04 .1600000E+04 .1800000E+04
.2400000E+04 .1415950E+03 .2261546E+03 .2996453E+03 .4350457E+03
.5991722E+03 .7794058E+03 .5900800E+00 .5923100E+00 .5945800E+00
.5968800E+00 .5980400E+00 .6015400E+00 .5378600E+00 .5398500E+00
.5418900E+00 .5439600E+00 .5450000E+00 .5481600E+00 .4986100E+00
.5004600E+00 .5023300E+00 .5042600E+00 .5052300E+00 .5081700E+00
.4381900E+00 .4398700E+00 .4415800E+00 .4433100E+00 .4441900E+00
.4468400E+00 .3802700E+00 .3817900E+00 .3833400E+00 .3849100E+00
.3857000E+00 .3881000E+00 .3252600E+00 .3266200E+00 .3280000E+00
.3294000E+00 .3301000E+00 .3322400E+00
*
***** Absorption X-Section Table
*
.4000000E+03 .8000000E+03 .1200000E+04 .1600000E+04 .1800000E+04
.2400000E+04 .1415950E+03 .2261546E+03 .2996453E+03 .4350457E+03
.5991722E+03 .7794058E+03 .5089000E-01 .5057300E-01 .5026600E-01
.4996700E-01 .4982000E-01 .4939000E-01 .5237200E-01 .5205300E-01
.5174400E-01 .5144300E-01 .5129500E-01 .5086200E-01 .5353000E-01
.5320900E-01 .5289500E-01 .5259300E-01 .5244400E-01 .5200800E-01
.5542800E-01 .5510600E-01 .5479300E-01 .5448800E-01 .5433800E-01
.5389800E-01 .5744400E-01 .5711600E-01 .5679900E-01 .5649000E-01
.5633800E-01 .5589200E-01 .5972300E-01 .5938600E-01 .5905900E-01
.5874000E-01 .5858300E-01 .5812200E-01
*
***** Fission X-Section Table
*
.4000000E+03 .8000000E+03 .1200000E+04 .1600000E+04 .1800000E+04
.2400000E+04 .1415950E+03 .2261546E+03 .2996453E+03 .4350457E+03
.5991722E+03 .7794058E+03 .2736097E-01 .2715214E-01 .2694950E-01
.2675363E-01 .2665772E-01 .2637649E-01 .2805652E-01 .2784258E-01
.2763665E-01 .2743720E-01 .2733911E-01 .2705215E-01 .2858027E-01
.2836320E-01 .2815297E-01 .2795044E-01 .2785100E-01 .2756113E-01
.2938063E-01 .2916184E-01 .2895035E-01 .2874416E-01 .2864291E-01
.2834761E-01 .3015435E-01 .2993270E-01 .2971797E-01 .2950973E-01
.2940705E-01 .2910713E-01 .3092586E-01 .3069935E-01 .3047976E-01
.3026466E-01 .3016016E-01 .2985157E-01

```

```

*
***** Nu-Fission X-Section Table
*
.4000000E+03 .8000000E+03 .1200000E+04 .1600000E+04 .1800000E+04
.2400000E+04 .1415950E+03 .2261546E+03 .2996453E+03 .4350457E+03
.5991722E+03 .7794058E+03 .6824100E-01 .6773100E-01 .6723900E-01
.6676100E-01 .6652700E-01 .6584100E-01 .6988600E-01 .6936700E-01
.6886500E-01 .6837900E-01 .6814000E-01 .6744100E-01 .7112200E-01
.7059600E-01 .7008400E-01 .6959100E-01 .6934900E-01 .6864100E-01
.7300500E-01 .7247300E-01 .7195900E-01 .7145800E-01 .7121200E-01
.7049200E-01 .7482200E-01 .7428100E-01 .7376000E-01 .7325200E-01
.7300300E-01 .7227300E-01 .7662500E-01 .7607300E-01 .7553800E-01
.7501700E-01 .7476100E-01 .7401100E-01
*
***** Xe Macroscopic X-Section Table
*
.4000000E+03 .8000000E+03 .1200000E+04 .1600000E+04 .1800000E+04
.2400000E+04 .1415950E+03 .2261546E+03 .2996453E+03 .4350457E+03
.5991722E+03 .7794058E+03 .1664600E-02 .1649500E-02 .1634600E-02
.1619700E-02 .1612400E-02 .1590700E-02 .1670900E-02 .1656500E-02
.1642200E-02 .1628100E-02 .1621100E-02 .1600400E-02 .1677000E-02
.1663000E-02 .1649000E-02 .1635200E-02 .1628500E-02 .1608400E-02
.1687400E-02 .1673800E-02 .1660400E-02 .1647100E-02 .1640600E-02
.1621200E-02 .1699200E-02 .1685900E-02 .1672800E-02 .1659900E-02
.1653500E-02 .1634700E-02 .1717500E-02 .1704300E-02 .1691300E-02
.1678500E-02 .1672100E-02 .1653500E-02
*
***** Xe Microscopic X-Section Table
*
.4000000E+03 .8000000E+03 .1200000E+04 .1600000E+04 .1800000E+04
.2400000E+04 .1415950E+03 .2261546E+03 .2996453E+03 .4350457E+03
.5991722E+03 .7794058E+03 .9948900E+06 .9852900E+06 .9757900E+06
.9664200E+06 .9618000E+06 .9481500E+06 .1035600E+07 .1026600E+07
.1017700E+07 .1008900E+07 .1004600E+07 .9917300E+06 .1067000E+07
.1058400E+07 .1049800E+07 .1041400E+07 .1037200E+07 .1024800E+07
.1115800E+07 .1107600E+07 .1099600E+07 .1091600E+07 .1087700E+07
.1076000E+07 .1163900E+07 .1156100E+07 .1148400E+07 .1140900E+07
.1137100E+07 .1126100E+07 .1215100E+07 .1207700E+07 .1200300E+07
.1193100E+07 .1189500E+07 .1178900E+07
*
***** Assembly Disc. Factor Table - W
*
.4000000E+03 .8000000E+03 .1200000E+04 .1600000E+04 .1800000E+04
.2400000E+04 .1415950E+03 .2261546E+03 .2996453E+03 .4350457E+03
.5991722E+03 .7794058E+03 .2000240E+01 .2000220E+01 .1999820E+01
.1999190E+01 .1998830E+01 .1997670E+01 .1937410E+01 .1938040E+01
.1938250E+01 .1938130E+01 .1938050E+01 .1937650E+01 .1891960E+01
.1893060E+01 .1894070E+01 .1894390E+01 .1894490E+01 .1894540E+01
.1825310E+01 .1826650E+01 .1827580E+01 .1828350E+01 .1828700E+01
.1829460E+01 .1764750E+01 .1766590E+01 .1767840E+01 .1768890E+01
.1769360E+01 .1770510E+01 .1733150E+01 .1734930E+01 .1736380E+01
.1737660E+01 .1738240E+01 .1739930E+01
*
***** Assembly Disc. Factor Table - S
*
.4000000E+03 .8000000E+03 .1200000E+04 .1600000E+04 .1800000E+04
.2400000E+04 .1415950E+03 .2261546E+03 .2996453E+03 .4350457E+03
.5991722E+03 .7794058E+03 .1224460E+01 .1222540E+01 .1220880E+01
.1219410E+01 .1218730E+01 .1216800E+01 .1233010E+01 .1231280E+01
.1229780E+01 .1228520E+01 .1227890E+01 .1226150E+01 .1239920E+01
.1238310E+01 .1236610E+01 .1235410E+01 .1234850E+01 .1233340E+01
.1250150E+01 .1249030E+01 .1248070E+01 .1247110E+01 .1246640E+01
.1245400E+01 .1261390E+01 .1260380E+01 .1259660E+01 .1259000E+01
.1258680E+01 .1257860E+01 .1281000E+01 .1280490E+01 .1280010E+01
.1279550E+01 .1279330E+01 .1278640E+01
*
***** Detector Flux Ratio Table
*
.4000000E+03 .8000000E+03 .1200000E+04 .1600000E+04 .1800000E+04
.2400000E+04 .1415950E+03 .2261546E+03 .2996453E+03 .4350457E+03
.5991722E+03 .7794058E+03 .9891800E+00 .9897800E+00 .9902490E+00

```


.9906670E+00	.9908580E+00	.9913620E+00	.9857230E+00	.9863100E+00	
.9867780E+00	.9872670E+00	.9874640E+00	.9880020E+00	.9837410E+00	
.9841210E+00	.9846150E+00	.9850500E+00	.9852510E+00	.9858490E+00	
.9804520E+00	.9810280E+00	.9815250E+00	.9819210E+00	.9820960E+00	
.9826270E+00	.9779290E+00	.9784330E+00	.9788730E+00	.9792580E+00	
.9794350E+00	.9799850E+00	.9753380E+00	.9758340E+00	.9762490E+00	
.9765660E+00	.9767320E+00	.9771570E+00			
*					
*****	Detector Microscopic X-Section Table				
*					
.4000000E+03	.8000000E+03	.1200000E+04	.1600000E+04	.1800000E+04	
.2400000E+04	.1415950E+03	.2261546E+03	.2996453E+03	.4350457E+03	
.5991722E+03	.7794058E+03	.1342130E+01	.1338480E+01	.1335320E+01	
.1332550E+01	.1331270E+01	.1327590E+01	.1355250E+01	.1351980E+01	
.1349130E+01	.1346820E+01	.1345640E+01	.1342370E+01	.1364460E+01	
.1361380E+01	.1357840E+01	.1355570E+01	.1354500E+01	.1351690E+01	
.1376000E+01	.1373870E+01	.1371990E+01	.1370120E+01	.1369200E+01	
.1366820E+01	.1387590E+01	.1385490E+01	.1384050E+01	.1382700E+01	
.1382050E+01	.1380400E+01	.1414840E+01	.1413680E+01	.1412610E+01	
.1411580E+01	.1411090E+01	.1409530E+01			
*					
*****	Effective Delayed Neutron Yield in 6 Groups				
*					
.1703595E-03	.1021614E-02	.9344275E-03	.2033880E-02	.7323374E-03	.1772451E-03
*					
*****	Decay Constants for Delayed Neutron Groups				
*					
.9571060E-02	.2381817E-01	.9017845E-01	.2398291E+00	.1049847E+01	.2932571E+01
*					
*****	Inv. Neutron Velocities				
*					
.5767301E-07	.2513322E-05				
*					